Nanoscale

ROYAL SOCIETY OF CHEMISTRY

REVIEW

View Article Online
View Journal | View Issue

Cite this: *Nanoscale*, 2024, **16**, 12793

Emergence of graphene as a novel nanomaterial for cardiovascular applications

Paniz Memarian,†[a,b] Zohreh Bagher,†[c,d] Sheida Asghari,[e] Mina Aleemardani *[f,g] and Alexander Seifalian *[a]

Received 2nd January 2024,
Accepted 1st June 2024

DOI: 10.1039/d4nr00018h

rsc.li/nanoscale

Cardiovascular diseases (CDs) are the foremost cause of death worldwide. Several promising therapeutic methods have been developed for this approach, including pharmacological, surgical intervention, cell therapy, or biomaterial implantation since heart tissue is incapable of regenerating and healing on its own. The best treatment for heart failure to date is heart transplantation and invasive surgical intervention, despite their invasiveness, donor limitations, and the possibility of being rejected by the patient's immune system. To address these challenges, research is being conducted on less invasive and efficient methods. Consequently, graphene-based materials (GBMs) have attracted a great deal of interest in the last decade because of their exceptional mechanical, electrical, chemical, antibacterial, and biocompatibility properties. An overview of GBMs' applications in the cardiovascular system has been presented in this article. Following a brief explanation of graphene and its derivatives' properties, the potential of GBMs to improve and restore cardiovascular system function by using them as cardiac tissue engineering, stents, vascular bypass grafts,and heart valve has been discussed.

1. Introduction

Cardiovascular diseases (CDs) are the leading cause of death worldwide.[1,2] Among the most common diseases in this category are myocardial infarctions (MIs) and strokes, which can permanently and irreversibly damage the heart muscle.[2,3] In spite of recent advances in therapeutic interventions, such as balloon angioplasty, bypass grafts, revascularization surgery, and pharmacological treatments, all challenges and limitations for each method to restore the function of injured heart muscles have not yet been overcome.[4–8] A potential solution to address these shortcomings is to develop engineered 3-dimensional (3D) cardiac tissue, which has drawn scientists' interest in conducting several research studies on a variety of synthetic and natural biomaterials in order to develop the desired structure.[5,9] There are several factors that should be considered for using biomaterials in cardiac applications, including mimicking native tissue constructions, providing chemical, mechanical, and electrical properties, as well as ensuring biocompatibility and hemocompatibility.[10–12] Previous studies indicate that carbon-based biomaterials are one of the most promising biomaterials in cardiac applications due to their exceptional properties.

Among all the allotropes of carbon, graphene (G) has gained extensive attention and is extensively used in biomedical applications. Due to its two-dimensional (2D) structure, which is composed of a single layer of hybridized sp2 carbon atoms arranged in a honeycomb lattice pattern and long-range conjugation bonds, it represents extraordinary physical and chemical properties, such as, 100 times superior mechanical properties than steel, light weighted, excellent electrical and thermal conductivity, and high surface area.[13–15] Several studies show that G has good biocompatibility in a specific range and antibacterial properties as well.[16–21] Different synthesis methods have been used to create GBMs to include a range of properties. These methods have been extensively reviewed and summarized from multiple perspectives, particularly emphasizing the scalable production, classification, and application of GBMs.[22,23] There are two types of

[a]*Nanotechnology and Regenerative Medicine Commercialization Centre, London BioScience Innovation Centre, London, UK. E-mail: alex@nanoregmed.com, p.memarian48@gmail.com, a.seifalian@gmail.com; Tel: +447985380797*
[b]*Department of Biomedical Engineering, Amirkabir University of Technology, Tehran, Iran*
[c]*ENT and Head and Neck Research Center and Department, The Five Senses Health Institute, School of Medicine, Iran University of Medical Sciences, Tehran, Iran. E-mail: baharebagher@gmail.com*
[d]*Department of Tissue Engineering & Regenerative Medicine, Iran University of Medical Sciences, Tehran, Iran*
[e]*Life Sciences and Biotechnology, Shahid Beheshti University, Tehran, Iran. E-mail: sh.asghari24@gmail.com*
[f]*Biomaterials and Tissue Engineering Group, Department of Materials Science and Engineering, Kroto Research Institute, The University of Sheffield, Sheffield, S3 7HQ, UK. E-mail: maleemardani1@sheffield.ac.uk*
[g]*Department of Translational Health Science, Bristol Medical School, University of Bristol, Bristol BS1 3NY, UK. E-mail: mina.aleemardani@bristol.ac.uk*
†These authors contributed equally to this work.

strategies for synthesizing G, top-down and bottom-up. The top-down approach includes mechanical or chemical exfoliation; through the process of exfoliation, a few layers of bulk material are separated from adjacent layers by overcoming the strong van der Waals attractions.[24,25] The bottom-up approach consists of pyrolysis or epitaxial growth of G and the chemical vapor deposition (CVD) process, as shown in Fig. 1. Pyrolysis decomposes carbon precursors like methane to synthesize G directly, while epitaxial growth deposits G on crystalline substrates such as silicon carbide for controlled alignment and high-quality synthesis. The CVD method enables the production of large-scale, high-quality G layers by promoting carbon atom self-organization on crystal surfaces through thermal hydrocarbon decomposition, followed by monolayer segregation on metal substrates.[25–29]

G also has some drawbacks limiting its use in biomedicine; these include its hydrophobic nature, unstable chemical structure, and incompatibility in some ranges. In order to address these concerns, G derivatives, including graphene oxide (GO), reduced graphene oxide (rGO), and functionalized graphene oxide (FGO), have been developed.[15,30,31] The atomic structure of GO is similar to that of G, but it has a more hydrophilic structure with a larger number of functional groups, such as carboxyl, hydroxyl, and epoxy groups.[31] The reduction of GO by thermal, chemical, or electrochemical treatments results in the production of rGO, which has fewer oxygen function groups and better conductivity.[32] Additionally, functionalization of GO with amine groups makes FGO.[30]

This review focuses mainly on the development of graphene-based materials (GBMs) for cardiac tissue applications. The study summarizes some of the most important cardiovascular disease research that has been conducted so far, as well as classifying some of the most common treatment methods, such as cardiac tissue engineering, vascular grafts, stents, and heart valves.

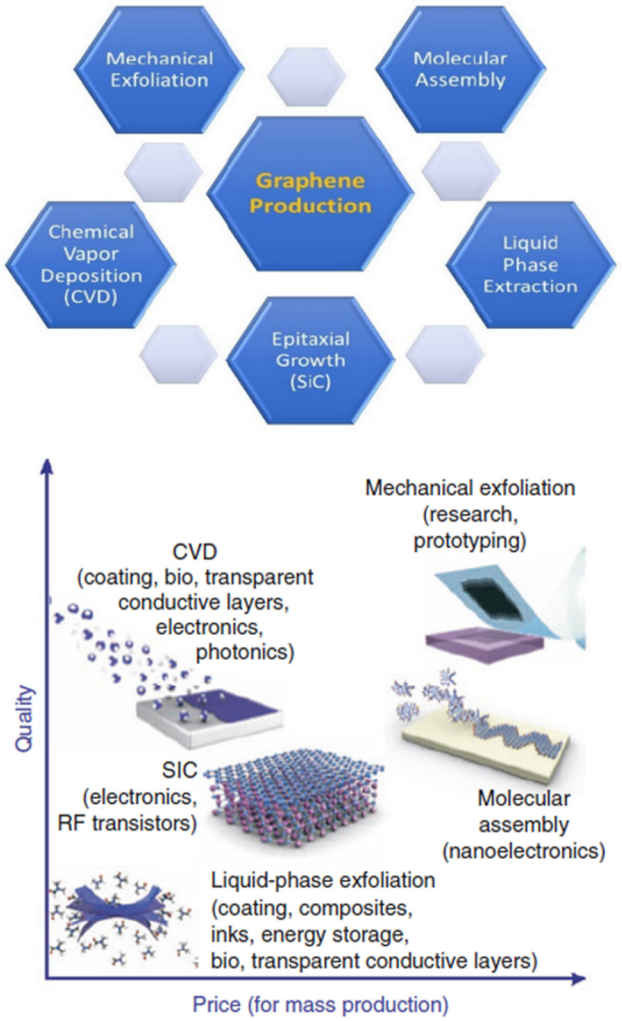

Fig. 1 Various methods of graphene production. Reproduced from ref. 189 and 254 with permission from [MDPI] and [Nature], copyright [2022] and [2012].

2. The properties of GBMs

The mechanical characteristics of the heart muscle are crucial due to its continuous load-bearing nature. The native myocardium has a Young's modulus and tensile strength ranging from 0.2–0.5 MPa and 3–15 kPa, respectively.[33–35] Studies suggest that GBMs with their mechanical features could serve as promising materials for reinforcing scaffolds in cardiovascular systems. The unique honeycomb structure of G, with carbon atoms arranged in sp^2 hybrid form, contributes to its exceptional mechanical properties, including a Young's modulus, fracture strength, and elastic modulus in the range of 1 TPa, 130 GPa, and 32 GPa, respectively.[36,37] The strong C–C bonding in G also results in a hardness higher than that of diamond.[36] However, factors such as GBMs' dispersion can negatively impact the uniformity of their mechanical structures. Overcoming issues like sheet van der Waals interactions and surface energy by applying parallel and perpendicular counter forces is crucial to inhibit G sheet aggregation and ensure proper dispersion.[38] Parameters such as solvent properties, the presence of functional groups, and the hydrophobic nature of the G family must be considered to achieve optimal dispersion. Studies have indicated that the dispersity of GO is higher than rGO and pristine G (GO > rGO > G), possibly due to the presence of oxygen-containing functional groups.[38–40]

As the hydrophobicity of GBMs increases, the need for using surfactant to enhance dispersity also rises. While surfactants have been shown to efficiently improve GBMs' dispersity, their potential cytotoxicity necessitates careful removal post-dispersion.[38] Other methods such as microwave heating, shear mixing, surface modification, and sonication can also aid in improving dispersity.[40–43] For instance, studies have shown that G quantum dots and low oxygen-containing GO exhibit better dispersion when subjected to microwave heating. Sonication has been found to be more effective for dispersing rGO, GO, and pristine G, with the duration of sonication

playing a crucial role. Shear mixing has shown more promising results for dispersing pristine G compared to sonication.[39,40] Surface modification through covalent and non-covalent methods is another viable approach to improving GBMs' dispersity, with covalent techniques demonstrating more promising outcomes in preserving stability during prolonged circulation and showing better loading capacity.[40,44]

The native myocardium functions by generating its own electrical signals at a rate of 60–100 times per minute, which are then propagated throughout the heart tissue, allowing the myocardium to function as a single unit.[45] The conductivity of the tissue is approximately 5×10^{-5} S cm^{-1} across and 1.6×10^{-3} S cm^{-1} along the tissue.[33,46] Any disruption in the cell signaling pathway can lead to alterations in ion-channel activities, resulting in heart dysfunctions.[47,48] To address issues related to disrupted cell signaling pathways, electroconductive materials have emerged as a novel approach for use in cardiovascular applications. Various studies have explored the use of electroconductive biomaterials such as polypyrrole (PPy), polyaniline, poly(3,4-ethylenedioxythiophene), and carbon nanomaterials.[49] Among electroconductive materials, GBMs have garnered much attention from researchers due to their electrical conductivity and their ability to facilitate intracellular coupling. The π–π conjugation system and presence of free electrons in G structures provide superior electrical conductivity (~10^4 S cm^{-1}) and unique charge carrier properties for GBMs, making them highly suitable for various biomedical applications.[50]

In addition to their conductivity, the high volume-to-surface ratio of GBMs makes them ideal candidates for use in electrical and electrochemical sensors.[51] They can effectively bond to ions and molecules, acting as receptors to detect specific molecules. For example, during ischemic stroke or myocardial infarction (MI), the levels of platelet-derived microparticles significantly increase, and a GO-based sensor could accurately identify patients at high risk based on these biomarkers.[52]

Another remarkable property of GBMs is their ability to absorb radiation, particularly near-infrared rays (NIR), and convert it into heat.[44] This characteristic makes GBMs suitable for applications in photothermal therapy, where cancer cells can be targeted and killed through hyperthermia.[53] GBMs' stability under NIR for extended periods makes it a promising technique for fabricating cardiac patches and applying them in clinical settings through minimally invasive surgical methods.[54]

In addition to their photothermal properties, GBMs also exhibit antibacterial and antioxidant properties. The antibacterial properties of G family materials are influenced by factors such as size, number of layers, and functional groups.[51,55,56] At the molecular level, GBMs' antibacterial features may be attributed to two mechanisms: physical disruption of bacterial membranes by their sharp edges and chemical mediation of oxidative stress, leading to bacterial cell death.[57,58] While combining GBMs with other antibacterial agents has shown potential to enhance antibacterial activities, research on the antibacterial properties of GBMs for cardiovascular applications is relatively limited.[33,59] Furthermore, GBMs demonstrate antioxidant properties due to their sp2 hybridization structures.[60] In the context of myocardial infarction (MI), where levels of reactive oxygen species (ROS) and proinflammatory cytokines increase in the injured area, the use of antioxidant agents such as GBMs can effectively reduce the excess ROS, thereby decreasing myocardial and vascular cell death and promoting the healing and remodeling processes.[33,61] This antioxidant property of GBMs holds promise for mitigating the detrimental effects of oxidative stress in cardiovascular conditions.

The bio and hemocompatibilities of GBMs are crucial and challenging aspects in their biomedical applications. Extensive studies have been conducted to evaluate the cytotoxicity of G materials, yet a consensus has not been reached on this topic. The toxicity of GBMs is influenced by various factors, including size, charge, number of layers, oxygen content, hydrophilicity, dose, dispersity, exposure duration, and specific applications.[33,50,51,62] The exact mechanisms underlying the cytotoxicity of GBMs remain unclear, but five possible routes have been proposed: generation of reactive oxygen species (ROS), depletion of mitochondrial membrane potential (MMP), cell starvation, physical damage, and genotoxicity.[40,63–67] One effective strategy to enhance the biocompatibility of GBMs is through functional modification, which can help adjust the aforementioned parameters and reduce the risk of cellular toxicity.[44,67–69] Given GBMs are inorganic nanomaterials, they have inherent resistance to self-degrade by the biological system.[38] Such modifications could modulate their biodegradability, effectively prevent bioaccumulation in tissues, thereby mitigating potential long-term toxicity risks associated with GBM exposure.[38,70] Tailoring GBMs' properties also positively impact the angiogenic properties, leading to positive impacts on angiogenic properties.[71–75] This enhancement can promote endothelial cell proliferation and migration, ultimately facilitating the formation of new blood vessels—a critical step in tissue remodeling and regeneration processes. In the subsequent sections, various examples of utilizing functionalized GBMs and investigating their bio and hemocompatibility have been further examined. These studies have demonstrated significant potential in promoting tissue regeneration, enhancing vascularization, and potentially addressing cardiovascular conditions through cutting-edge biomedical applications.

Fig. 2 presents a concise schematic representation of the distinctive characteristics of GBMs that are paramount in the realm of cardiovascular research. Drawing upon existing literature, the figure also delineates several prevalent fabrication methodologies commonly employed in this field.

3. Incorporation of GBM in tissue-engineered scaffolds for cardiac tissue

3.1. Cardiac tissue engineering

The heart has insufficient capability to self-repair and regeneration due to the limited number and growth of heart tissue

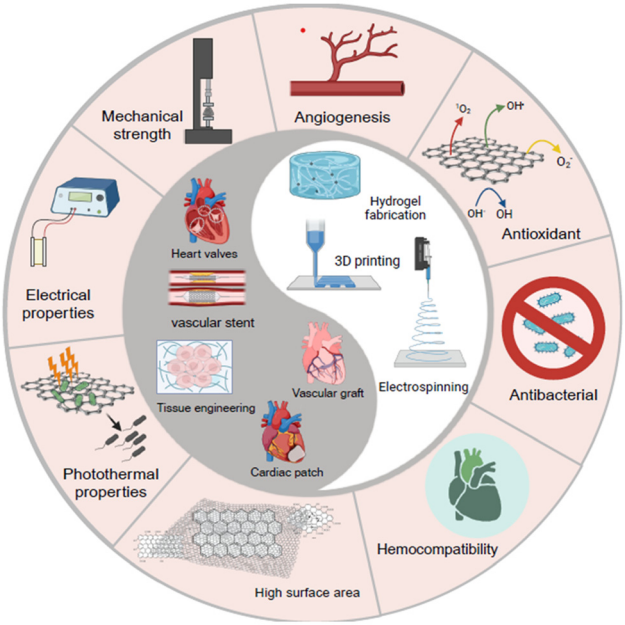

Fig. 2 Highlights the techniques, characteristics, and uses of graphene in cardiovascular applications.

stem cells.[76,77] In the realm of scientific inquiry, cardiac tissue engineering has emerged as a promising avenue for restoring function at injured sites and improving blood flow, thereby potentially reducing the necessity for heart transplants, invasive procedures, and mortality rates.[48,77,78] Despite ongoing efforts, the development of fully functional cardiac tissue through cardiac tissue engineering remains a challenge, necessitating careful consideration of various factors before clinical application, including the provision of native-like physical, mechanical, and chemical cues for cultured cells.[48,79] Studies have revealed that cardiac muscles exhibit an electrical conductivity, with electrical signals being generated and propagated 60–100 times per minute.[45,48] The myocardium's organized myofibers contribute to its unique structural design, offering essential mechanical support for the rhythmic and spontaneous contractions of the heart.[45,78,80] Therefore, the selection of suitable biomaterials in cardiac tissue engineering is critical for constructing and engineering the microarchitecture of native myocardium, facilitating the alignment and elongation of cells, as well as restoring cardiac conductivity, contractility, uniform tissue structure, and function.[33,81,82]

While a variety of biocompatible natural and synthetic polymers have been utilized in engineering cardiac tissues resembling the native myocardium's microarchitecture, challenges persist regarding topography, biophysical, chemical, and mechanical properties.[83–87] GBMs, known for their exceptional mechanical, electrical, and biocompatible properties, hold promise in meeting these critical requirements for mimicking cardiac tissue and enhancing the expression of cardiac-specific genes and proteins, including TrPT-2, Actn4, connexin 43, among others.[30,31,33,80,88–95]

3.1.1. Cardiac patch mechanical properties. In various studies, GBMs have been combined with other substances to enhance their mechanical properties within the desired range for cardiac tissue applications. For instance, Ferreira *et al.* utilized GBMs as nanofillers to augment the tensile properties of PEG hydrogels, resulting in stiffer and stronger hydrogels suitable for load-bearing and blood-contact devices.[96] They employed GBMs with different characteristics such as thickness, lateral size, and oxidation degree: the reduced form of few-layer G (FLG), GO, and few-layer GO (FLGO). TEM images revealed that FLG and FLGO had larger lateral sizes compared to GO. The impact of the oxidation degree was also assessed, with FLG (3.2% oxidation degree) exhibiting agglomeration in aqueous media due to its low oxygen content, unlike GO and FLGO with higher oxidation degrees (32.6% and 34.6% oxidation degree). Interestingly, FLGO significantly enhanced the stiffness and tensile strength of the hydrogel, with improvements of up to 115% and 196%, respectively; while, FLG did not reinforce hydrogel, underscoring the influence of oxidation degree on the mechanical properties of the hydrogel. By considering factors like viscosity, homogenization ability, and degassing, the maximum feasible concentrations for dispersing GO and FLGO with PEG were determined. The addition of 1% FLGO and 4% GO led to substantial changes in the young modulus of the PEG hydrogel from 26 ± 11 kPa to 163 ± 17 and 76 ± 9.5 kPa, respectively. It was found that the ultimate tensile strength (UTS) and elongation at break results were significantly improved in samples containing 4% w/v GO (16-folds higher than neat hydrogel and 126 ± 16% of initial size), suggesting 4% w/v GO provided better mechanical properties. The cytocompatibility of GBMs was evaluated using HUVECs, confirming their non-cytotoxic nature and anti-adhesive properties towards HUVECs, platelets, and *S. aureus*, indicating their potential safety for blood-contact devices. A similar study was conducted by incorporating GBMs into Poly (2-hydroxyethyl methacrylate) (pHEMA).[17] The properties of pHEMA/GBM composites with varying oxidation degrees, lateral sizes, and thicknesses were evaluated. The study reported that oxidized GBMs could provide more effective mechanical reinforcement compared to non-oxidized GBMs. When oxidized GBMs were used, the Young's modulus of the composite increased from 0.744 to 1.80 × 10^3 kPa, whereas non-oxidized GBMs did not significantly alter the Young's modulus. A similar trend was observed for the ultimate tensile strength (UTS), where the oxidized sample showed a 4.4-fold increase to 678 kPa, while the non-oxidized sample maintained around 150 kPa. This improvement in mechanical properties with oxidized GBMs could be attributed to better interaction and uniform distribution of the oxidized forms of GBMs within the composite. The establishment of hydrogen bonds with oxygen-containing groups may lead to fewer rupture points and overall better mechanical properties. Furthermore, the thickness of the GBMs can also impact the Young's modulus. Thinner GBMs, such as GO, were found to be more efficient fillers based on the results. However, it is worth noting that there are contradictory findings in other

studies regarding the use of GBMs for mechanical reinforcement. Despite potential concerns about increased surface roughness with higher GO content leading to elevated platelet and bacteria adhesion in some studies, the composite in this research maintained its anti-adhesive, anti-bacterial, and anti-thrombotic properties due to the prevailing characteristics of pHEMA. *In vivo* assessments confirmed the hemocompatibility of the pHEMA/GO composite, demonstrating even lower platelet adhesion than ePTFE, a common material for vascular access, suggesting its suitability for cardiovascular devices.

In contrast to studies focusing on hydrogels with high modulus, such as the work by Burdic *et al.*,[97] this study proposed a soft injectable hydrogel with fatigue resistance and adequate conductivity for transmitting mechanical and electrical signals to coordinate myocardial tissue contraction.[46] The hydrogel was created by combining PEGDA700-Melamine (PEG-MEL) with GO (Fig. 3). The resulting hydrogel exhibited a young modulus of 25 Pa and demonstrated enhanced conductivity due to the π–π conjugation, surpassing the conductivity of PEGDA hydrogel (PEG-MELL/GO: 2.84×10^{-4} S cm^{-1}, PEGDA: 3.47×10^{-9} S cm^{-1}). Moreover, this hydrogel displayed excellent cytocompatibility, and when adipose tissue-derived stromal cells (ADSCs) were encapsulated within it, the cells maintained their initial spindle shape. In an *in vivo* experiment involving MI rat models, the injection of this hydrogel led to improvements in ejection fraction (EF) and fractional shortening (FS). The GO-incorporated hydrogel also exhibited superior neovascularization compared to other samples. Furthermore, the results indicated that PEG-MELL/GO hydrogels reduced infarction size and fibrosis area, suggesting a promotion of cardiac function recovery.

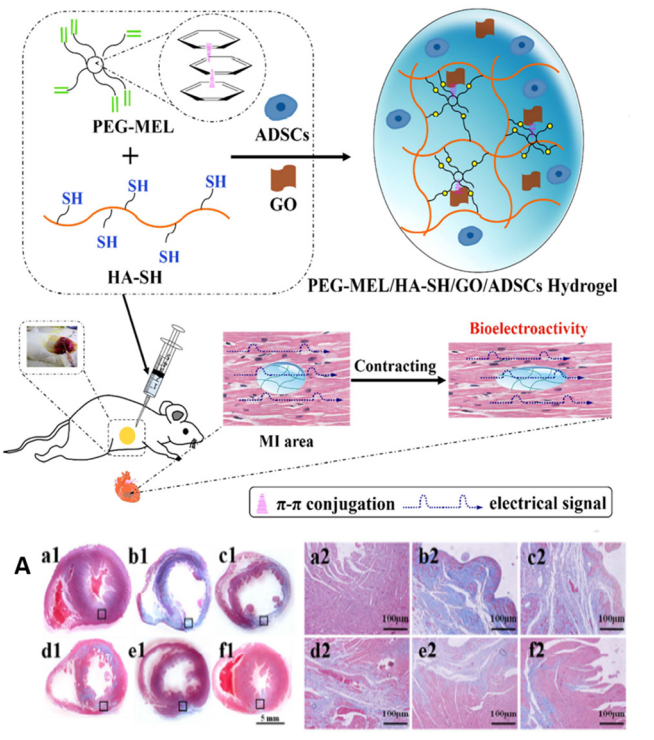

Fig. 3 Schematic illustration of PEG-MEL/HA-SH/GO hydrogel system encapsulating ADSCs for cardiac repair. (A) Cardiac repair by different treatments after 28 days (Masson's trichrome staining for collagen (blue) and muscle (red)). Reproduced from ref. 46 with permission from [Elsevier], copyright [2017].

3.1.2. Cardiac patch electrical properties. The heart is an electroactive tissue responsible for propagating electrical signals throughout the entire organ, resulting in heartbeats and the synchronized response of cardiomyocytes (CMs).[10] When constructing engineered cardiac tissue, it is crucial to provide an electroactive substrate to mimic the cellular environment and replicate cell-cell or cell-matrix interactions.[98] GBMs exhibit excellent electrical properties, and their incorporation with other materials can facilitate appropriate coupling between scaffolds and cardiac tissue.

In a study, gelatin methacryloyl (GelMA) hydrogel was fabricated by incorporating rGO at concentrations of 0, 1, 3, and 5 mg mL^{-1}.[99] Previous research has suggested that gelatin can act as a biocompatible surfactant for the suspension of G due to van der Waals and π–π stacking interactions. This property of GelMA helps inhibit the agglomeration of rGO, resulting in a homogeneous hydrogel containing rGO. The incorporation of rGO led to a significant improvement in the mechanical and electrical properties of the hydrogel, with a Young's modulus of 22.6 kPa and an impedance value of 4 kΩ. Biocompatibility evaluations demonstrated that the rGO/GelMA hydrogel was non-toxic to cardiac cells. Additionally, the expression of cardiac markers α-actinin and Cx-43 indicated that the rGO-containing hydrogel provided a structure with better organization and cell-cell coupling, leading to proper contractile properties. *In vivo* assessments revealed that cardiomyocytes on rGO-GelMA hydrogels exhibited greater contractility, a faster spontaneous beating rate, and better biological activities compared to pure GelMA hydrogels. The study suggested that higher electrical conductivity and structural uniformity of the hydrogel could create an appropriate environment for cardiomyocytes, improving charge redistribution and propagation of action potential, thereby promoting synchronized beating throughout the engineered cardiac tissue. The results of this study were promising, and rGO has since garnered attention for cardiac tissue engineering applications, particularly in the development of cardiopatches, due to its ability to mimic cardiac properties effectively.

In another study, researchers aimed to replicate the anisotropic electrical signal propagation observed in the native myocardium by using aligned and random electrospun silk fibroin functionalized with rGO (rGO/silk$_{A/R}$) as depicted in Fig. 4.[100] The conductivity of the rGO/silk$_{A/R}$ patches was found to be significantly higher parallel to the aligned nanofibers compared to perpendicular to them. The conductivity ratios in the parallel direction were 1.7, which closely matched the native myocardial anisotropic conductivity range of 1.1–2.6. After four weeks of implanting the patches, the isotropic conductive rGO/silk$_{A/R}$ patches demonstrated remarkable repair of the infarcted myocardium and alleviated adverse myocardial remodeling. This was evidenced by a reduction in scar size,

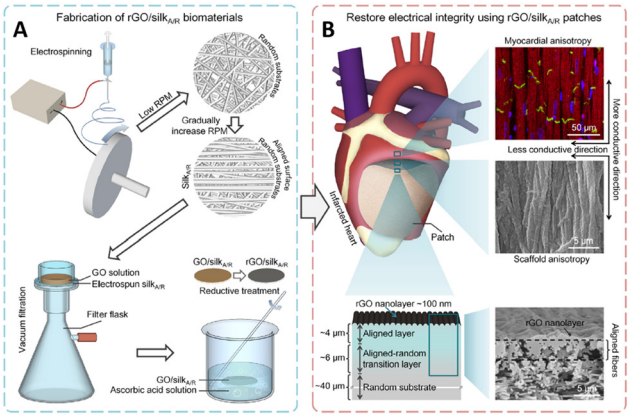

Fig. 4 Schematics illustrating the fabrication of rGO/silk A/R scaffolds: (A) fabrication of aligned and random rGO/silk scaffold by electrospinning method and then deposition in GO solution through vacuum-filtration; (B) cross-sectional SEM images demonstrating the structure of the rGO/silk$_{A/R}$ scaffolds consisting of a random, aligned-random, aligned nanofibrous layer, providing anisotropic conductive cardiac patch. Reproduced from ref. 100 with permission from [Elsevier], copyright [2022].

decreased susceptibility to arrhythmias, improved left ventricular wall thickness, enhanced cardiomyocyte survival, and increased capillary angiogenesis. The outcomes of the study highlighted the potential of the anisotropic conductive rGO/silk$_{A/R}$ biomaterial as a promising candidate for reconstructing the electrical myocardial microenvironment following myocardial infarction. This biomaterial could play a crucial role in restoring the electrical properties of the heart tissue post-infarction and potentially improve overall cardiac function and remodeling.

GO, has also gained much attention in several cardiac patch studies.[92] In a study, GO-gold nanosheets (GO-Au) were incorporated into a chitosan solution at concentrations of 0.1%, 0.25%, and 0.5% w/v to create a conductive and biodegradable patch.[101] The addition of GO-Au resulted in a two-fold increase in conductivity, exceeding 10×10^{-5} S cm^{-1}, while maintaining controlled swelling and degradation properties. After 5 weeks of implantation, the patch showed significant improvements in average QRS intervals and the QRS complex. Moreover, the implanted patches enhanced cardiac tissue function and electrical coupling by notably increasing fractional shortening, ejection fraction, left ventricular diameter dimensions, expression of Cx43, cardiac contractility, and the heart's ability to pump blood more efficiently, suggesting the enhance of the conductivity of the patch make it a promising candidate for applications in cardiac tissue engineering and myocardial repair.

Hydrogel containing oligo (polyethylene glycol) fumarate (OPF) incorporated with varying concentrations of GO were synthesized (0.3, 0.6, and 1.0 mg mL^{-1} GO/OPF).[89] The addition of GO to the scaffolds resulted in a significant improvement in electrical conductivity, with the highest concentration achieving a 4-fold increase, reaching 4.235×10^{-3} S cm^{-1}. The GO-loaded hydrogel showed enhanced adhesion of rat cardiac fibroblast cells compared to the control group. Four weeks after implantation, the GO nanoparticles facilitated the expression of intercalated disk (ID) related proteins such as N-cadherin (NC), plakoglobin (PG), and desmoplakin (DP), which play crucial roles in cardiac function and integrity. The OPF samples treated with GO exhibited improved gap junction remodeling, as evidenced by the increased expression levels of related genes (Cx43, Cx40, Cx37, and Cx45). This enhancement was attributed to the presence of GO, which was found to elevate the phosphorylation levels of GSK-3β (pGSK-3β), subsequently activating β-catenin signaling and leading to an upregulation of Cx43 expression as displayed in Fig. 5. Furthermore, the treated samples showed a reduction in scar tissue and an increase in myocardial tissue within the infarcted area, indicating improved heart structure and functional recovery. The OPF-GO samples also exhibited higher mRNA levels for smooth muscle actin (SMA) and vascular endothelial growth factor (VEGF), suggesting positive angiogenic effects potentially associated with the enhancement of gap junctions (Fig. 6). These results were attributed to the presence of an electrically conductive network within the hydrogel, highlighting the potential of GO-incorporated OPF hydrogels for cardiac tissue engineering applications.[89,102]

3.1.3. Cardiac patch biological properties. The cytotoxicity and hemocompatibility of cardiovascular devices are critical considerations to prevent blood coagulation and immune system responses.[103–105] The contradictory findings in studies utilizing GBMs underscore the complex interplay of factors influencing the hemocompatibility, cytotoxicity, and anticoagulation mechanisms of biomaterials in blood-contacting devices.[17,106–108] Parameters such as surface energy, charge, roughness, GBM concentrations, dispersity, and other factors play crucial roles in determining the biocompatibility of these materials. For example, some studies suggest that increased surface roughness, charge, and energy can enhance platelet adhesion and thrombogenicity, while others have reported contrasting results, emphasizing the need for thorough evaluation and optimization of GBMs for clinical applications in cardiovascular devices.[109–113]

Study by Kayat *et al.* have highlighted the potential for GBMs, particularly GO, to induce cell and tissue damage, especially in organs like the heart and liver, potentially leading to inflammation and fibrosis.[114] This can occur due to the distribution of GBMs in these organs, triggering local and systemic inflammatory responses.[115,116] Furthermore, research by Kanakia *et al.* has indicated that high concentrations of G (over 250 mg mL^{-1}) can lead to histopathological changes.[117] Functionalizing GBMs with different agents and functional groups, such as polyethylene glycol (PEG), aptamers, antibodies, enzymes, and magnetic nanoparticles, has been proposed as a promising strategy to enhance their applications and mitigate negative effects in bio-applications.[118–122]

In a study aimed at reducing the cytotoxicity of GO, researchers utilized Arginine (Arg), Lysine (Lys), and Ginsenoside Rh2 (Rh2) to functionalize GO, creating nano-

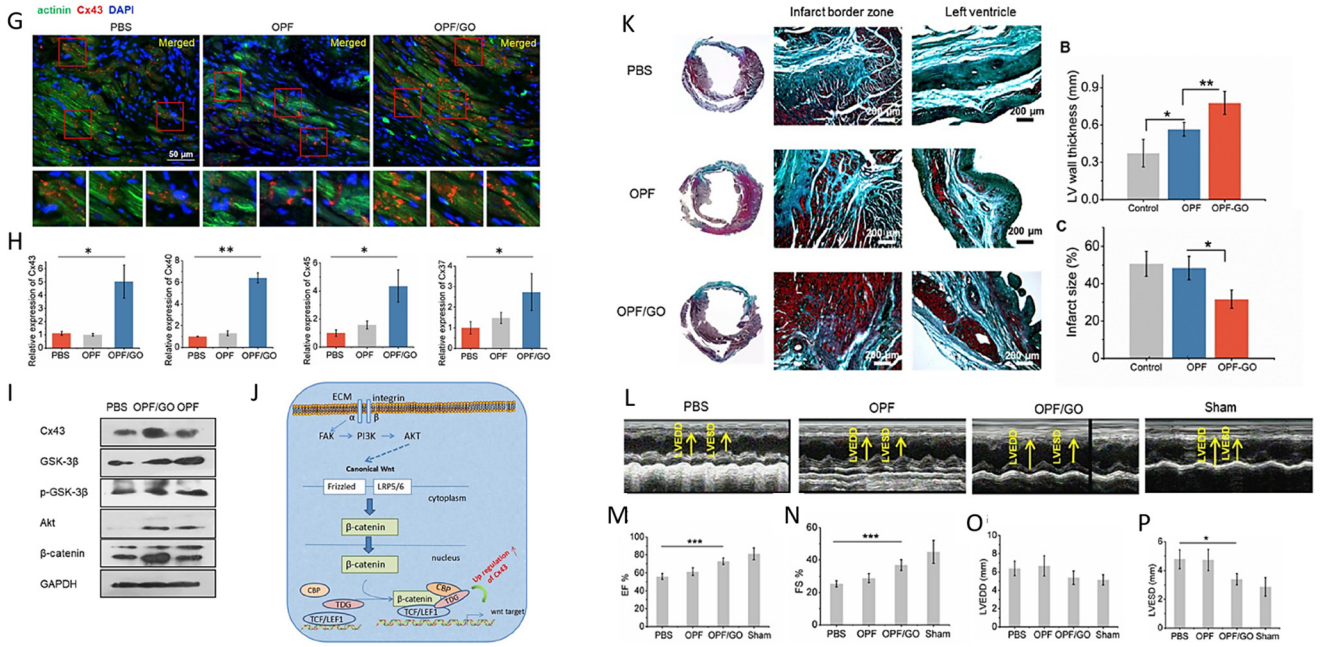

Fig. 5 (G, H, I and J) The formation of gap junction-associated proteins and their mechanism in the infarcted region. (K, L, M, N, O and P) Masson's trichrome staining and echocardiographic measurements demonstrating the effects of OPF/GO hydrogel on the morphology and myocardial functional recovery of infarcted hearts. Reproduced from ref. 89 with permission from [Springer], copyright [2019].

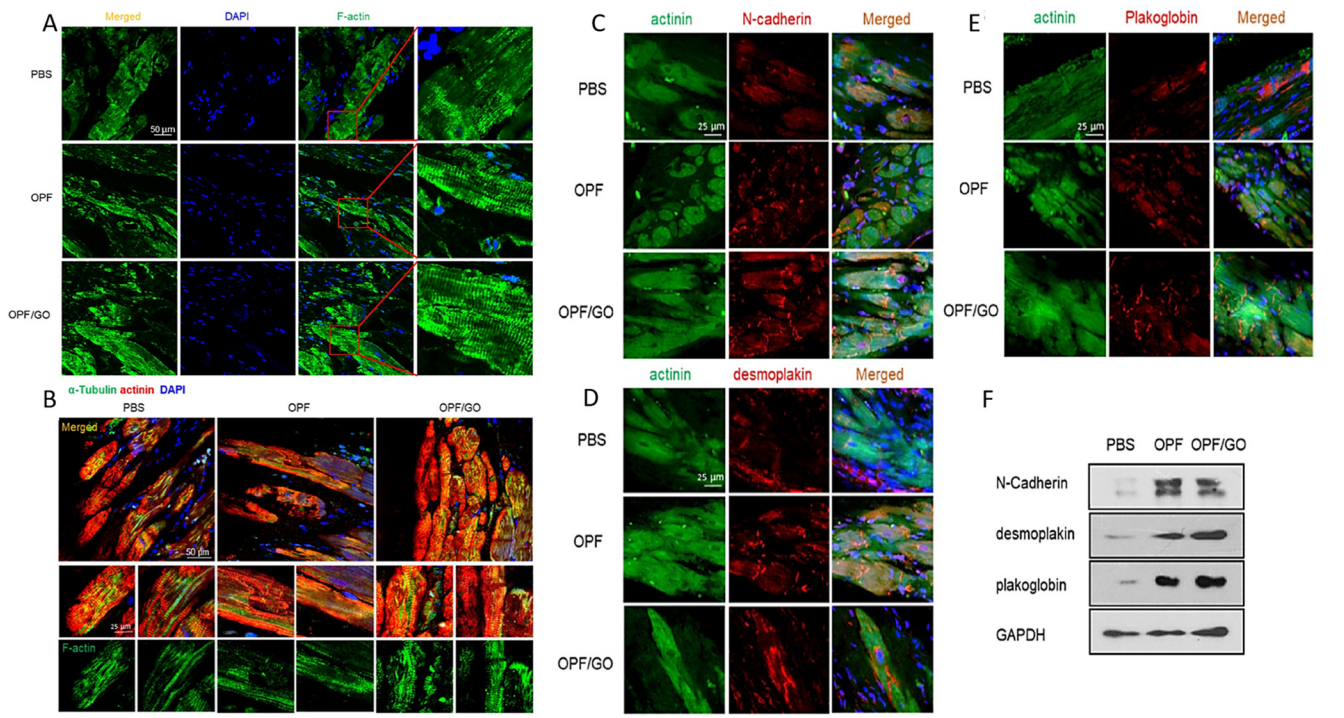

Fig. 6 (A and B) OPF/GO enhanced cytoskeletal structure 4 weeks after MI. (C, D, E and F) Immunofluorescence staining and western blot results of ID-related proteins in the hearts of PBS-, OPF-, OPF/GO-injected groups at 4 weeks post MI. Reproduced from ref. 89 with permission from [Springer], copyright [2019].

structures with excellent anti-cancer activity.[122] The results demonstrated that functionalizing GO with hydrophilic groups could enhance cytotoxicity and hemocompatibility. By incorporating Arg and Lys, the nanostructure size was increased, and the surface charge was improved, reducing the interaction between the negative charge of GO and the positive charge of

phosphatidylcholine in red blood cells (RBCs).[123] This led to a decrease in RBC toxicity and hemolytic activity. The anticancer activity of these nanostructures was assessed using the childhood acute lymphoblastic leukemia (ALL) cancer cell line (K562), revealing that GO-Arg-Rh2 and GO-Lys-Rh2 exhibited the highest anticancer activity. In rat models injected with these nanostructures at GO concentrations of 200 and 1000 mg mL^{-1}, histological examination of heart tissue showed that the presence of Rh2 resulted in a decrease in side effects on the heart tissue and blood system, typically associated with chemotherapy for blood cancers, highlighting the potential of these nanostructures in mitigating such side effects.

Minimally invasive surgery (MIS) is gaining attention in the medical field due to its potential to reduce mortality rates, shorten recovery times, and decrease operation durations.[124,125] In a recent study, researchers developed a near-infrared (NIR)-triggered self-unfolding microneedle (MN) patch made of GO-poly (vinyl alcohol) (GO-PVA) with varying mass ratios (0%, 0.2%, 0.4%, 0.8%, and 1.6%) loaded with vascular endothelial growth factor (VEGF) as shown in Fig. 7.[54] The utilization of GO, known for its excellent absorption in the NIR region, endowed the patch with a remarkable shape memory effect and enhanced VEGF loading and release efficiency.[126] Biocompatibility assessments using rat cardiomyocytes derived from H9c2 cells revealed low cytotoxicity and over 80% cellular viability. The 0.8% GO-PVA sample, chosen for its optimal mechanical strength, controllable local sustained drug release, and good biocompatibility, was implanted into rats with MI. A week post-implantation, significant improvements were observed, including increased neovascularization (confirmed by CD31 and VEGF staining), anti-inflammatory effects, reduced scar size, and decreased levels of a-SMA, VWF, and collagen-1. Statistical analyses demonstrated superior left ventricular ejection fraction (LVEF) and left ventricular short-axis shortening rate (LVFS) compared to the control group, indicating promising prospects for MIS applications.

3.1.4. Cardiac patch and angiogenic properties. In the field of tissue engineering, a significant challenge is the absence of vascular networks essential for providing continuous oxygen and nutrients to cells, crucial for their survival. A recent advancement involves the development of vascularized conductive elastic cardiac patches by incorporating holey GO/poly (3,4-ethylenedioxythiophene) polystyrene sulfonate (hGO/pPy) at different mass ratios (1 : 0.5, 1 : 1, 1 : 3, or 1 : 5) into a poly (hydroxyethyl methacrylate) cryogel, followed by reduction into p(HEMA)-rhGO/pPy cryogels (HrhGPs).[127] Among the samples tested, the formulation containing pPy/hGO at a ratio of 0.5 : 1 w/w demonstrated excellent mechanical and electrical properties comparable to native myocardium, with a Young's modulus of 31.59 ± 0.44 kPa and an electrical conductivity of 0.071 ± 0.013 S m^{-1}. Biocompatibility assessments revealed that HrhGP0.5 supported the survival of over 80% of CMs and exhibited favorable cytocompatibility. A 3D biomimetic vessel structure was created in the patch using a coronary artery casting as a template as depicted in Fig. 8, which was subsequently removed after cryopolymerization. Rat aortic endothelial cells (RAECs) were seeded inside and outside the channels under dynamic conditions to establish fully vascularized channels (v-HrhGP0.5). Co-culturing CMs in v-HrhGP0.5 (v-HrhGP0.5 ECP) demonstrated enhanced CM functionalization and synchronous contraction. *In vivo* evaluations showed a 1.5-fold increase in microvessels and arterioles, with substantial anastomoses formed between v-HrhGP0.5 ECP and host vessels, promoting electrical integration and conduction velocity in the infarcted heart. Furthermore, RNA sequencing analyses indicated that the conductive and dynamic microenvironment created by v-HrhGP0.5 ECP enhanced the repair of myocardial infarction (MI) by upregulating mRNA expression related to cardiac muscle contraction and ATP biosynthesis.

Numerous studies have been conducted to improve angiogenesis in tissue engineering.[128–132] However, G-based materials were shown to upregulate the expression of angio-

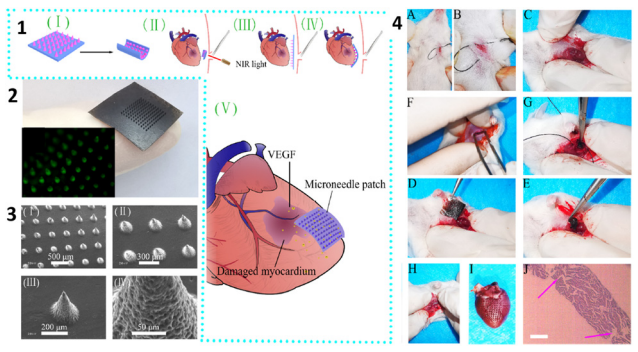

Fig. 7 A general view and various steps of the MIS for treating MI with GO-PVA microneedle patches (1 and 4). The SEM image of the patch and microneedles morphology (2 and 3). Reproduced from ref. 54 with permission from [ACS], copyright [2021].

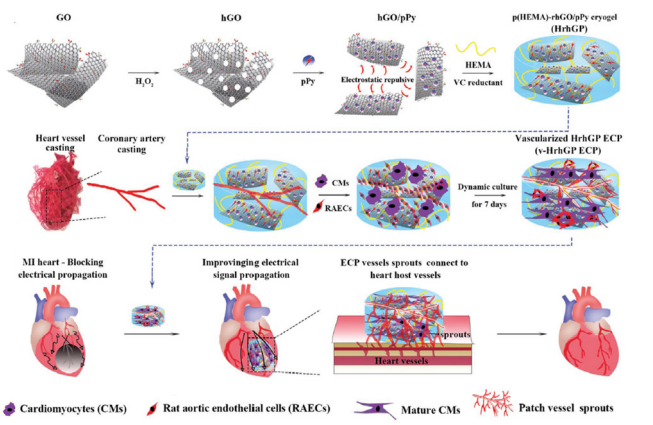

Fig. 8 The preparation process of the vascularized conductive elastic ECP and its effect after implantation in MI rats; (1) using the incorporation of rhGO/pPy and poly (HEMA) to fabricate HrhGPs cryogel after reduction and cryopolymerization; (2) preparation of v-HrhGP and culturing of CMs and RAECs; (3) the patches were implanted into the MI hearts of rats, and their efficacy was explored. Reproduced from ref. 127 with permission from [Wiley], copyright [2022].

genic genes, including CD34, MMP9, SDF-1, and VEGF, and positively promote angiogenesis.[71,129,131,133] In a study involving polyvinyl alcohol and carboxymethyl cellulose scaffolds loaded with varying concentrations of rGO nanoparticles (0.0025%, 0.005%, 0.0075%, 0.01% w/v), it was observed that during cell culture, the rGO-loaded scaffolds seeded with endothelial cells (EA. hy926) did not exhibit cytotoxic effects or morphological changes.[129] Moreover, the presence of rGO nanoparticles led to an increase in the proliferation rate of the cells. In an *in vivo* chick chorioallantoic membrane assay, it was found that the number of blood vessels significantly increased when the concentration of rGO exceeded 0.0075% (w/v) by 62%, according to Fig. 9. This phenomenon, known as arteriogenesis, was also observed during the assay period, as the average thickness of the vessels increased by 51.7%, indicating blood vessel maturation.[129,134] In another study, the angiogenic effects of GO were investigated by analyzing angiogenic-related gene expression (biocompatibility). A chitosan-GO hydrogel was synthesized by freezing and lyophilization technique.[135] The study showed that the incorporation of GO (up to 150 mg L^{-1}) improved the uniformity of the hydrogel structure and enhanced its mechanical properties. Specifically, the elastic modulus, tensile strength, and elongation at the break increased from 0.829 to 22.026 MPa, from 1.363 to 7.153 MPa, and from 61.3% to 161.5%, respectively. When GO was added to endothelial progenitor cells (EPCs) extracted from umbilical cord blood, it led to enhanced tube formation and angiogenesis. Western blot analysis of angiogenesis-related genes revealed an upregulation of CD34, VEGF, MMP9, and SDF-1 in the GO-loaded hydrogel. This suggests that GO may influence the angiogenic ability of EPCs through the SDF-1/VEGF signaling pathway.[135–137]

Norahan *et al.* conducted a study where they fabricated scaffolds based on collagen that were covalently coated with various concentrations of GO (5, 15, 30, 45, 75, 90 μg ml^{-1}).[10] The scaffolds exhibited randomly oriented interconnected pores with GO flakes properly distributed in the pore walls. To enhance the biocompatibility of the scaffolds, monolayer GO flakes with a lateral size of about 300–500 nm and a thickness of 2 nm were used, as studies have indicated lower cytotoxicity and inflammation response of nano-sized GO compared to micro-sized GO.[138] Mechanical and electrical analyses showed that with increasing concentrations of GO, the tensile strength, Young's modulus, and electrical conductivity of the scaffold increased. For example, the tensile strength and Young's modulus increased from 75 kPa and 160 kPa for Col-GO-5 to 162 kPa and 750 kPa for Col-GO-90, respectively. Although GO itself did not exhibit high conductivity, the electrical conductivity was altered from $3.8 \pm 0.09 \times 10^{-4}$ S m^{-1} for Col-rGO-5 to $29 \pm 0.18 \times 10^{-4}$ S m^{-1} for Col-rGO-90 after reduction. Biocompatibility results indicated that both Col-GO-90 and Col-rGO-90 significantly enhanced cell proliferation rate and adhesion, with no observed cytotoxicity on human umbilical vein endothelial cells (HUVECs) due to the surface properties and interaction of functional groups on GO and rGO, leading to the adsorption of serum proteins. Gene expression evaluation on rat neonatal cardiomyocytes (CMs) revealed that the expression of cardiac markers such as Cx43 and Actn-4 increased approximately two-fold in Col-rGO-90 samples compared to Col samples, while the expression of TrpT-2 was upregulated 3.2-fold, indicating an improvement in extracellular matrix-cell interactions. Furthermore, the optimal sample (Col-rGO-90) was subcutaneously implanted in mice, showing higher cell migration and newly formed blood vessels, highlighting the angiogenic characteristics of GO (Fig. 10).

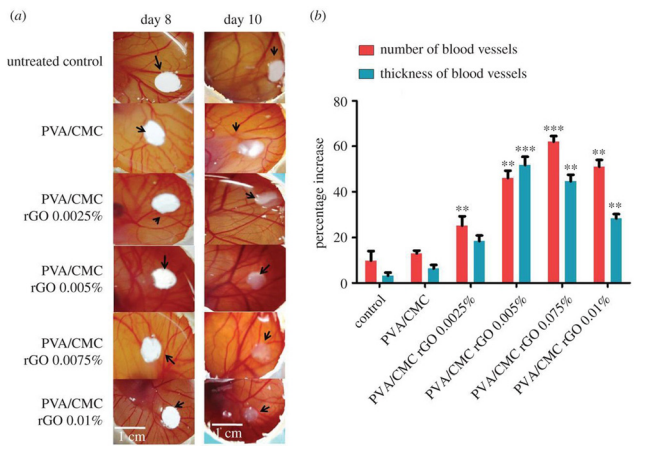

Fig. 9 (a) Image of chick chorioallantoic membrane assay; (b) The percentage of number and thickness of blood vessels. Reproduced from ref. 129 with permission from [Royal Society open science], copyright [2018].

While GBMs have been extensively studied for their angiogenic effects, some studies have suggested that they could also act as anti-angiogenic agents and play a role in tumor growth and metastasis by targeting angiogenic markers.[139,140] In certain studies, G and its derivatives have been shown to activate macrophages and dendritic cells, leading to the stimulation of the immune system to produce cytokines that can effectively target cancerous cells.[139] For example, a study on bovine serum albumin-capped GO demonstrated that it can strongly bind to VEGF-A, a crucial proangiogenic factor, and inhibit its function.[141] This blocking of VEGF-A suppresses angiogenic signaling processes in chick chorioallantoic cells and hinders neovascularization in rabbit corneal cells, making it a potential therapeutic anti-angiogenic agent.[141] Furthermore, in another study, GO was incorporated into a nanocomposite with monoclonal antibodies (mAbs) targeting FSHR, a marker of tumor vasculature expressed during the early stages of tumor metastasis.[140] This approach shows promise in targeting tumor vasculature and inhibiting metastatic spread.

3.1.5. Cardiac patch and stem cells. Stem cell therapy is a promising approach for treating damaged heart tissue after a myocardial infarction (MI). However, transplanting cells into the infarcted area poses several challenges. Factors such as the cell environment and conditions during the injection process can lead to cell differentiation or damage before reaching the targeted area. Additionally, poor adhesion of cells to the tissue

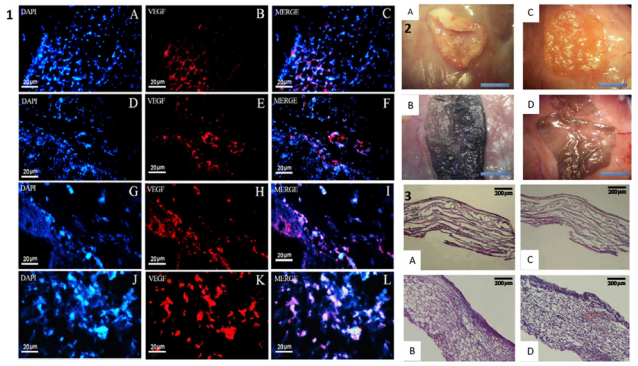

Fig. 10 (1) Immunohistology analysis of Col and Col–rGO of scaffolds after implantations; (2) and (3): morphology and H & E staining of the scaffolds after 2 (A and B) and 4 (C and D) weeks after subcutaneous implantation. Reproduced from ref. 10 with permission from [Wiley], copyright [2019].

and the risk of cells leaking to other sites are concerns that need to be addressed.[142–144] To overcome these limitations, using a biomaterial matrix that can provide a favorable microenvironment for the cells may be an effective strategy. This approach can help create a supportive environment for the transplanted stem cells, promoting their survival and function in the desired location.[98,144–147] Mesenchymal stem cells (MSCs) are a promising type of stem cell commonly used in cardiac tissue engineering. MSCs have the ability to differentiate into cells of mesodermal, ectodermal, or endodermal origin, making them versatile for regenerating damaged cardiac tissue. Studies have shown the potential of MSCs in improving cardiac function and promoting tissue repair after MI.[147–152]

In a study investigating the optimal niches for human umbilical cord-derived mesenchymal stem cells (hUC-MSCs), the effect of GO flake sizes (100–200 nm, 0.2–2 μm) and the reduction level of rGO (low and high) with different thicknesses (5, 10, 15, and 25 μg cm^{-2}) was evaluated.[32] The study found that increasing the size of GO flakes enhanced cell proliferation by up to 17% in aqueous and 14% in ethanol solutions. Additionally, the number of hUC-MSCs improved at lower levels of rGO reduction. However, increased thicknesses of both GO and rGO induced oxidative stress, leading to the generation of reactive oxygen species and activation of apoptosis. The study identified 10 and 15 μg cm^{-2} as the most suitable thicknesses. Furthermore, due to their hydrophilic properties, GO-based substrates were found to facilitate MSC migration in terms of cell speed and distance. While cells adhered more rapidly to GO samples than to rGO samples initially, after 2, 3, and 4 hours, cells adhered to both types of samples similarly. The study also revealed that the expression levels of angiogenic-related genes GATA-2, ENDOGLIN, and VE-CADHERIN were significantly elevated with both GO and rGO compared to control groups. Moreover, both GO and rGO promoted capillary formation as well as differentiation into cardiomyocyte and endothelial-like cells. Interestingly, the study found that GO did not require any external factors to differentiate into angiogenic cells, whereas rGO did. Additionally, both GO and rGO increased the expression levels of cardiomyogenic genes, such as GATA-4 and ACTC1, and myocyte-specific markers (ME22C) without the need for biological induction of differentiation.

In a recent study, human bone marrow mesenchymal stem cells (hBM-MSCs) were encapsulated in conductive hydrogels composed of alginate (ALG) and reduced rGO.[98] These hydrogels were then implanted into rat models with chronic ischemic cardiomyopathy. The results of the study showed significant improvements in various cardiac parameters in rGO-ALG-MSC group compared to the control group and other treatment groups. Specifically, the rGO-ALG-MSC group exhibited enhanced fractional shortening (FS), ejection fraction (EF), wall thickness, and internal diameters, indicating improved cardiac function and structure. Morphological observations revealed increased blood vessel formation, particularly in the rGO-ALG-MSC group, 8 weeks post-transplantation. Histological analyses further supported the positive outcomes, showing reduced collagen fibrosis and increased neovascularization in the group treated with rGO-ALG-MSC. These findings suggest that the use of rGO/ALG hydrogel encapsulated with BMSCs is both safe and effective for the treatment of myocardial infarction, offering promising results for cardiac repair and regeneration. In another study, a hybrid composite of collagen type 1, which is the most abundant protein in the body, and G at concentrations of 8% and 32% by weight was evaluated.[153] The study demonstrated that as the G content increased, the stiffness and electrical conductivity of the scaffold significantly increased. The enhanced hydrophilicity and roughness of the scaffold due to the presence of G led to increased cell adhesion, with improvements of 26% and 45% observed for samples with 8% and 32% G content, respectively. Furthermore, the addition of G resulted in a reduction in bacterial cell binding to the surface by up to 17.6%. In addition to these findings, the study applied 48 hour external electrical stimulation at 25 V cm^{-1} and 1 Hz. The results, as indicated by immune fluorescent staining of sarcomeric myosin (MF20) and cardiac troponin (cTNT), showed that the addition of G improved the cross-striation structure and alignment of cells. This enhancement further promoted the elongation, maturation, and alignment of embryonic stem cell-derived cardiomyocytes (ESC-CMs), suggesting that the hybrid composite scaffold has the potential to support and enhance the development of functional cardiac tissue (Table 1).

3.2. Vascular stents and grafts

Vascular diseases are among the leading causes of death around the globe.[166] With increasing demands for curing these diseases, various vascular therapeutic strategies have been developed, including percutaneous and surgical revascularization procedures.[167] Stent implantation as an advanced part of these protocols has drawn scientists' attention since 1980.[168] Nowadays, there are three distinct generations of stents: bare metal stents, drug-eluting stents, and bio-

Table 1 Application of cardiac patches with GBMs for regeneration of myocardium. Abbreviations: MP, mechanical properties; YM, young modulus; EC, electrical conductivity; CMs, cardiomyocytes; MFs, myocardial fibroblasts; HUVECs, human umbilical vein endothelial cells; hiPSC-CMs, human-induced pluripotent stem cell-derived cardiomyocytes; CPC, cardiac progenitor cells; hMSCs, human bone marrow mesenchymal stem cells; ADSC, adipose tissue-derived stromal cells; HCMs, human cardiac myocytes; EPC, endothelial progenitor cells; ESC, embryonic stem cell; SMCs, smooth muscle cells; RBC, red blood cells; CPA, cell proliferation and attachment; PCL, poly(caprolactone); PGS, poly(glycerol sebacate); polyethylene glycol Diacrylate, PEGDA; GelMA, gelatin methacryloyl; ↑ increase; ↓ decrease

Biomaterial(s)	Concentration of G	Fabrication technique	*In vitro* (cell type)	*In vivo* (animal model), duration	Outcomes	Year, Ref.
Polyurethane/rGO (PU/rGO)	5, 10, 15 and 20 wt%	Electrospinning and electrospraying	H9c2 and HUVEC	Not conducted	↑ Tensile strength ↑ H9c2 and HUVEC cells viability and attachment, particularly PU/RGO10 and PU/RGO15	2023, 154
Holey GO/ polypyrroleincorporated poly hydroxyethyl methacrylate	Hybrid suspension with a hGO to pPy mass ratio of 1 : 0.5, 1 : 1, 1 : 3, or 1 : 5	Cryogelation	CMs	MI rat model, 4 weeks	↑ Cell viability over 80% *In vivo*: ↑ microvessels and arterioles up to 1.5-fold ↑ Electrical integration and conduction velocity ↑ Cardiac muscle contraction and ATP biosynthesis mRNA express ↓ Infarcted area (~32%) ↑ cGMP-PKG signaling pathway ↑ Expression of functionalization-related genes	2022, 127
PGS and G	0.5, 1, 2, 4 (wt%)	Micropatterned film by solvent evaporation	H9c2 rat CMs	MI rat model, 4 weeks	Tensile strength (0.6 ± 0.1–3.2 ± 0.08 MPa) ↑ Conductive to 5.8×10^{-7} S m^{-1} promote cell proliferation in H9c2 *In vivo*: ↓ infarct size and degree of myocardial fibrosis ↓ Collagen deposition ↓ Left ventricular. ↑ Fractional shortening and ejection fraction ↑ CX43 protein expression	2022, 155
Poly (ethylene glycol) and few-layer GO (FLGO), or GO	1% w/v FLGO and 4% w/v GO	*In situ* crosslinking	HUVECs	Not conducted	↑ MP Optimum sample: 4% w/v GO Possess anti-adhesive and anti-bacterial properties No cytotoxicity	2022, 96
Alginate and GO	2 g	Dual cross linking	MSCs and L929 fibroblasts	Not conducted	↑ MP and toughness ↑ L929 cell viability and adhesion Regulate the fate of encapsulated MSCs ↑ MSCs differentiation markers (1.30-times for TNT and 1.21-times for GATA4)	2022, 156
rGO and Alginate	10 μg mL^{-1}	Using crosslinking agent	hBM-MSCs and CMs	Rat model of chronic ischemic cardiomyopathy, 8 weeks	↑ Cell viability ↑ Cardiac marker expression (TrpT-2, Conx43, and Actn4) *In vivo*: ↑ EF, FS, wall thickness ≫ ↑ cardiac function ↑ Formation of blood vessels	2022, 98
rGO and silk	0.01 mg rGO per 1 cm^2 patch	Electrospinning (aligned/random)	CMs and MFs	Acute MI rat model, 4 weeks	Anisotropic conductivity *In vivo*: ↑ repairing infarcted myocardium. ↑ Pumping function Thickened left ventricular walls. ↓ Susceptibility to arrhythmias ↑ CD31-positive microvessels ↓ density of α-SMA	2021, 100
PEGDA hydrogels and G nanoplatelets	15%	4D printing	hiPSC-CMs, hMSCs, and HUVECs	Not conducted	Dynamic and remotely controllable transformation in a spatiotemporal manner ↑ Rhythmic and directional beating behavior ↑ Myocardial protein (α-actinin and cTnI) expression of the nascent myocardial tissue ↑ Degree of alignment and elongation for hMSCs and hiPSC-CMs	2021, 157

Table 1 *(Contd.)*

Biomaterial(s)	Concentration of G	Fabrication technique	*In vitro* (cell type)	*In vivo* (animal model), duration	Outcomes	Year, Ref.
PCL/PGS/G	0.25, 0.75 and 1 wt%; Optimum: 1 wt%	Electrospinning	HCMs	Not conducted	↑ Tensile strength: 21.51 to 11.41 MPa cell clusters ↑ CPA ↑ Cell viability: 98.79% (≫1 wt%)	2021, 158
(GO)-poly (vinyl alcohol)-VEGF loaded	0, 0.2, 0.4, 0.8, and 1.6 wt%	Freeze–thaw	CMs derived from H9c2	MI mice model, 2 weeks	↑ Cellular viabilities >80% ↓ Expressed α-SMA, VWF, and collagen-1 *In vivo*: ↑ neovascularization ↑ New blood vessels ↓ Myocardial fibrosis	2021, 54
GO and Chitosan	0.1, 0.5, and 1.0 wt%	Using crosslinking agent and freeze dry	EPCs	Not conducted	↑ Hardness and strength ↑ The expressions of angiogenesis-related genes at optimum content of GO (CD34, VEGF, MMP9, and SDF-1) ≫ ↑ angiogenesis	2021, 159
Oxidized alginate (OA), myocardial extracellular matrix (ECM), and amine-rGO	25 μg ml^{-1}	Using crosslinking agent	HUVECs	Not conducted	↑ MP: 41.1 kPa ↑ EC: 2.8×10^{-4} S m^{-1} Well distributed amine-rGO ↑ Cell viability	2021, 160
pHEMA and GO	1% w/v	Using crosslinking agent	RBCs and HUVECs	porcine arteriovenous-shunt model, 30 min	MP (YM): 1.80×10^{3} kPa Possess anti-adhesion against HUVECs, bacteria, and platelets ↑ Hemocompatibility & cytocompatibility *In vivo*: ↓ Blood component adhesion	2021, 17
GO and rGO	5, 10, 15, or 25 μg cm^{-2}	Coating	hUC-MSCs	Not conducted	No change of phenotype, cell cycle progression ↑ Cell proliferation in sample with large flakes of GO ↑ Cardiomyogenic and angiogenic differentiation	2020, 73
Functionalized G (carboxyl group), PCL/chitosan/polyPyrrole (PCP) and heparin	0.5, 1.5, and 2.5 wt%	Electrospinning	ESC	Not conducted	↑ Hydrophilicity ↑ MP: 0.032 ± 0.001 to 0.098 ± 0.001 MPa ↑ EC: 1.12 ± 0.045 to 5.33 ± 1.16 S cm^{-1} ↓ Bovine serum albumin (BSA) adsorption (↑ hemocompatibility) Embryoid bodies (EB) formation Cardiomyocytes differentiation	2020, 161
Silk, GO, and growth factor	0.25 mg mL^{-1} and 0.5 mg mL^{-1}	Using gelation agent (PEG)	CPCs and CMs	MI mouse model	Uniform distribution of RGO and porous structure ↑ Cytocompatibility, cell adhesion and proliferation rate ↑ The expression of cardiac markers (SAC, Cx43 and cTnI) *In vivo*: ↑ LV wall thickness ↓ Scar thickness and infarct size ↓ Pro-inflammatory cytokines Positive effect on cardiomyocytes differentiations	2020, 162
rGO and collagen	200, 400, 600 and 800 μg ml^{-1}; Optimum: 400 μg ml^{-1}	Coating	HUVECs	Not conducted	↑ Cell viability Cardiac gene expression upregulation like Cx43, troponin-T and actinin-4 (≫400 μg ml^{-1}) ↑ MP: 340 ± 20 kPa ↑ EC: $2.2 \pm 0.3 \times 10^{-5}$ S m^{-1} Antibacterial properties	2019, 163
GO and polyethylene terephthalate (PET)	0.5 mg ml^{-1}	Electrospinning	HUVECs	Not conducted	Cardiomyocyte elongated and spreading morphology ↑ EC	2019, 164
Polyurethane and rGO	0% and 0.025% of PU	Electrospinning	Satellite cells from skeletal muscle	Not conducted	↑ MP and the fibers' orientation Well dispersion of rGO nanoparticles ↑ Cell growth and differentiation on aligned fibers ↑ The expression of Troponin I cardiac-specific gene on aligned fibers	2019, 88

Table 1 *(Contd.)*

Biomaterial(s)	Concentration of G	Fabrication technique	*In vitro* (cell type)	*In vivo* (animal model), duration	Outcomes	Year, Ref.
Gelatin, poly caprolactone (PCL), and G	0%, 0.3%, 0.5%, 0.8%, and 1% of Gt/PCL	Electrospinning	Neonatal rat ventricular CMs (NRVCMs) and CMs	subcutaneous in rat model, 6 weeks	Optimum sample: 0.5%G ↑ EC & ↑ MP ↑ Cell viability and adhesion *In vivo*: No cell necrosis and tissue damage	2019, 93
Chitosan and GO	50, 100, 150, 600 mg L^{-1}	Freezing and lyophilization technique	H9C2 rat MCs	Not conducted	Optimum sample: 150 mg L^{-1} GO ↑ Uniformity ↑ EC: 0.134 S m^{-1} ↑ Cell viability and proliferation ↑ The expression of CX-43	2019, 135
Polyvinyl alcohol, carboxymethyl cellulose, and rGO	0.0025%, 0.005%, 0.0075%, 0.01% w/v	Freezing and lyophilization technique	Endothelial cells (EA. hy926), fibroblasts (NIH3T3), and endothelial-like cells (ECV304)	Chick chorioallantoic membrane model, 10 days	No cytotoxicity and morphology change ↑ Proliferation rate *In vivo*: ↑ Angiogenesis and arteriogenesis	2018, 129
Chitosan and GO-Au	0.1%, 0.25%, 0.5% (w/v)	Freeze dry	SMCs, fibroblasts and hiPSC-CMs	MI rat model, 5 weeks	Two-fold increase in EC ↑ iPSC derived cardiomyocytes attachment *In vivo*: ↑QRS interval, conduction velocity and contractility in infracted zone ↑ connexin 43 levels	2018, 101
GO, Arginine, Lysine, and Ginsenoside Rh2	5, 25, 100, 200, 400, 1000 μg ml^{-1}	Esterification and radical reaction	RBCs and cancer cell line (K562)	Injection in rat model, 2 weeks	↑ Nanostructure size and charge ≫ ↓ toxicity to RBCs ≫ ↑Hemocompatibility & ↑ anti-cancer activity *In vivo*: ↓ Heart tissue damage	2018, 122
GO and Collagen	5, 15, 30, 45, 75, and 90 μg mL^{-1}	Freeze dry	HUVECs and rat newborn CMs	subcutaneous implantation on mice, 4 weeks	Well disperse GO ↑ MP (YM): 750 kPa & ↑UTS: 162 kPa EC: 29×10^{-4} S m^{-1} ↑ The expression of Cx43, Actn-4, and TrpT-2 ↑ Biocompatibility ↓ Cytotoxicity and inflammation reaction *In vivo*: ↑ Angiogenesis	2018, 10
Oligo (polyethylene glycol) fumarate (OPF) and GO	0.3, 0.6, and 1.0 mg mL^{-1} GO/OPF	Using crosslinking agent	Cardiac fibroblast cells	MI rat model, 4 weeks	↑ EC: 4.235×10^{-3} S cm^{-1} ↑Cell adhesion & no cytotoxicity *In vivo*: ↑ The expression of NC, PG, and DP ≫ ↑ cardiac function and integrity ↑ The expression of Cx43, Cx40, Cx37, and Cx45 ≫ ↑ gap junction remodeling ↑ Angiogenesis	2018, 116
PEGDA700-Melamine (PEG-MEL) and GO	0.5 mg ml^{-1}	Using crosslinking agent	ADSCs	MI rat model, 4 weeks	↑ EC: 2.84 × 10–4 S cm^{-1} MP: 25 Pa ↑ Cytocompatibility *In vivo*: ↑ EF, FS, and neovascularization ↓ Infarction size and fibrosis area	2016, 46
rGO and GelMA	0, 1, 3 and 5 mg ml^{-1}	Hydrogel fabrication	NIH-3T3 cells and rat CMs	Not conducted	↑ Tensile strength ↑ DNA content ⇒ no significant toxicity ↑ Cardiac markers expression	2016, 165
bovine serum albumin-capped GO (BSA/GO)	30, 100, and 150 μg mL^{-1}	Mixing	HUVECs	Chick chorioallantoic membrane and rabbit corneal neovascularization (CNV) models, 2 weeks	Strong bonding to VEGF-A ↑ Inhibition the proliferation, migration of cells and tube formation *In vivo*: ↓ blood vessel formation, growth, and density ≫ ↑ anti-angiogenic properties	2016, 141

degradable stents; however, they still have several major drawbacks, including the biocompatibility and hemocompatibility of biomaterials, their mechanical properties, and their design, which inhibit them from being considered as a long-term and completely successful clinical treatment.[169] To mitigate these adverse effects, stents must undergo various modifications to improve their properties and meet clinical requirements. G and its family are among the most sought-after materials due to their chemically inert nature, atomic smoothness, durability, and biocompatibility properties, which have been successfully used for surface or bulk stent modifications as shown in Table 2.[170,171]

Table 2 Abbreviations: HUVECs, human umbilical vein endothelial cells; HaCaT, Human keratinocyte; HUECs, human vascular endothelial cells; HUSMCs, human vascular smooth muscle cells; ECs, endothelial cell; CPAM, cell proliferation and migration; VSMCs, vascular smooth muscle cells; HPCAEC, human primary coronary artery endothelial cells; RAECs, rat aortic endothelial cells; RASMCs, rat aortic smooth muscle cells; RBCs, red blood cells; WBCs, white blood cells; Zn, zinc; Mg, magnesium; PTMC, poly (trimethylene carbonate); HEMA, 2-hydroxy ethyl methacrylate; RSL, resveratrol; EDOT, 3,4-ethylene dioxythiophene; PSS, polystyrene sulfonate; DA, dopamine; Hep, heparin; NiTi, Nitinol; ↑, high, greater or increase; ↓, less or decrease; ⇒, concluded or resulted in; ≫, higher than others

	Biomaterial(s)	Graphene-based materials concentration(s)	Technique	Target and cell type	Outcomes	Year, Ref.
Vascular stents	Zn/PEG grafted G nanoplatelets (GNPs)	25, 50, 100 mg L^{-1} of f-GNP	Zn/functionalized-GNP nanocomposite prepared by electro co-deposition (ECD)	HaCaT	↑ Compressive yield stress ranges from 182.3 ± 7.9 MPa (f-GNP: 25 mg L^{-1}) to 284.9 MPa (f-GNP: 100 mg L^{-1}) ↓ Friction coefficient and wear loss of Zn/f-GNP (100 mg L^{-1}) nanocomposites (58.1% and 47.36%) ↑ Antibacterial Performance (*S. aureus* and *E. coli*) ↑ CPAM	2022, 206
	AZ31b Mg/GO/PTMC	0, 0.2, 1, 3, 6, and 10 wt%	Spin coating	HUECs and HUSMCs	↑ Anti-corrosion ability (up to 6 wt%) ↓ Cytotoxicity ↑ CPAM ↓ Adhesive number of platelets ⇒ ↓ thrombosis risk Good blood compatibility Optimum: 6 wt% GO	2022, 207
	HEMA/methacrylate graphene oxide (MeGO) and loaded with RSL	0.1 g	3D printing	HUVECs	↑ Elastic stiffness of the stent (0.29 ± 0.01 × 10^{-2} MPa) ↑ NO release from HUVECs ⇒ Suppress platelet adhesion and activation No cytotoxicity ↓ Cell apoptosis (5-fold) ↓ TNF-α release ↓ H_2O_2-induced ROS ⇒ recover endothelial cell functions	2022, 182
	Mg alloy/chitosan functionalized GO (GOCS) loaded with Zn^{2+} and propranolol	1 mg mL^{-1} GO	Covalently immobilized coated by immersing in GOCS@Zn/Pro solution (1 mg mL^{-1})	ECs	↑ Corrosion resistance ↓ Degradation rate ↓ Platelet adhesion and activation ≫ ↑ hemocompatibility ↑ Clotting time ⇒ excellent anticoagulation ↑ Cell adhesion and proliferation ↑ Nitric oxide (NO) and VEGF Expression ⇒ ↑ surface endothelialization ↓Bacterial adhesion and proliferation	2020, 208
	AZ31B Mg alloy /chitosan-functionalized graphene oxide (GOCS)/hep	1 mg ml^{-1}	coated by immersing in GOCS and heparin solution	ECs	↓ pH value of solution ⇒ ↑ corrosion resistance ↑ Coating thickness ⇒ ↑ corrosion resistance ↓ Adhered platelets ↓ Hemolysis rate by multilayer coating ↑ CPAM ↑ Expression of VEGF and NO in endothelial cells ⇒ stimulates the growth of the endothelial cells ⇒ ↑cGMP in platelets ⇒ ↓ Intracellular Ca^{2+} ⇒ preventing the adhesion and activation of platelets and fibrinogen ↑ Blood compatibility	2020, 169
	SUS316L stainless steel/EDOT /GO/ PSS /Hep	0.01 g	Coated by electrochemically copolymerizing	Mouse embryonic fibroblasts (NIH 3T3 cells)	Exhibited anti-fouling ability ↓ Protein adsorption GO contributed most of the anti-adsorption effect ↑ Blood coagulation time No cytotoxicity	2019, 209
	316L stainless steel/DA/(GO) loaded with docetaxel (DTX)/carboxymethyl chitosan (CMC) loaded with Hep	2 mg ml^{-1}	Coated by ultrasonic spray system	VSMCs	↓ Hemolysis rate ↓ Adhered platelets appear to be spherical and inactivated No platelets and fibrin (after 12-week implantation) ⇒ ↑Antithrombotic ability No toxicity (zebrafish embryos and larvae) ↑ Inhibit the proliferation of VSMCs Inhibits intimal hyperplasia and thrombosis and promotes endothelialization (*in vivo* rabbit study)	2019, 210
	PCL-rGO	0.1, 0.3, 0.6, and 1.0% (wt/wt)	The 3D printing technique of melt electrowriting (MEW)	HUVECs	↑ Mechanical Properties (for 0.1% rGO: a 2.5-fold ↑Young's modulus (520 ± 39 MPa) and a 1.5-fold) ↑ Ultimate tensile strength (21 ± 2 MPa) ↑ CPAM ⇒ ↑endothelialization ↓ Platelet adhesion for 0.1% rGO	2019, 211
	Stainless steel/G/chitosan/TiO_2 nanoparticles (TiO_2NPs)	7(wt.%)	Coated by immersing in Ch-G-TiO_2NPs	RBCs and WBCs	No blood platelets adhesion when exposed to healthy and diabetic human blood No negative effect on RBCs and WBCs count	2018, 212
	Stainless steel (316L) coated by G	Not mentioned	Coated by using the PMMA-based transfer method	HPCAEC	↑ CPAM on G-overlaid discs over 100% No cytotoxic effect ↑ Metabolic activity ↓ Fibroblast phenotype cells ↑ Endothelium phenotype cells ↓ Platelets attached (two times) Diminishing the endothelial to mesenchymal transition ⇒ ↓ in-stent restenosis risk	2018, 213
	Pure titanium coated by DA and heparin-loaded GO	0.5 mg ml^{-1} GO solution	Coated by immersing into the GO solution	ECs	↑ Surface hydrophilicity ↑ CPAM ↓ Adhered platelets ↑ Blood compatibility ↑ Clotting time	2016, 214
	NiTi coated by G	Not mentioned	G layer Coated by using the PMMA-based transfer method	RAECs and RASMCs	↓ Stress gradients in cells ⇒ better cells morphology Supporting cells proliferation No cytotoxicity G coatings inhibit any charge transfer from fibrinogen (subsequent blood clotting) ⇒ ↓fibrinogen/albumin ratio ⇒ ↑ hemo-compatibility Hemo-compatibility of G is layer-independent.	2012, 170

Table 2 *(Contd.)*

	Biomaterial(s)	Graphene-based materials concentration(s)	Technique	Target and cell type	Outcomes	Year, Ref.
Vascular graft	Thermoplastic polyurethane (TPU)/GO	0%, 0.5%, 1%, and 2% of TPU	Electrospinning	HUVECs, Mouse fibroblast (3T3)	↑ Tensile modulus and tensile strengt ↑ CPAM ↑ Fibroblasts viability (0.5% GO) ↓ Water contact angle Oxygen plasma treatment ⇒ ≫ ↑hydrophilicity ↑ HUVECs attachment 0.5% GO scaffolds ≫ ↑ live cells ~(99% viability) 5% GO sample exhibited high flexibility ⇒ ↑ recovery from the cyclical force loading Proper suture retention strength for use in small-diameter vascular graft applications ↓ Platelets attached (round morphology) ⇒ ↓ thrombosis	2015, 215
	Polyvinyl alcohol (PVA)/G	1, 2, and 3 wt% OF PVA	Electrospinning	ECs	↓ Young's modulus from 65.3 to 42.7MPa ↑ Elongation (~3 times for 3% G) and tensile strength ↑ G concentration ⇒ ↑water contact angle and hydrophobicity No toxicity ↑ CPAM	2020, 216
	Decellularized Arteries (Human placental and umbilical cord tissues)/GO	0.5 mg ml^{-1}	Recirculating perfusion system	HUVECs	↑ Burst pressure of the umbilical cord decellularized arteries by 29%, strain by 25%, and compliance by 10% ↑ Compliance by 10% for placental chorion decellularized arteries ↓ Adhered platelets (both) ≫ in umbilical cord arteries ↓Bacterial adhesion	2021, 187
	Collagen-coated vascular matrix/apyrase and 5′-nucleotidase (5′-NT)/rGO	Not mentioned	Coated by dispersion in RGO-enzyme complexes	ECs	↑ Stability of the enzyme by binding to Rgo ↓ ADP concentrations ↑ AMP and adenosine ⇒ enzymes good activity and could transform ADP into antiplatelet AMP and adenosine ⇒ Inhibit platelet aggregation ↑ CPAM ↑ Patency rate of 90% in *in vivo* study	2017, 188
Heart Valve	Acellular pulmonary valve/rGO	100 μg ml^{-1}	Coated by immersing in rGO solution	Fibroblast cell	No effect on CPAM (indirect) No significant difference in platelet activation, adhesion, DNA fragmentation	2015, 1
	Functionalized GO (FGO)/poly (carbonate-urea) urethane (PCU) (the trade name Hastalex)/GORE-TEX	5% of prepolymer	Mixing	ECs (Ea.hy 926)	↑ Mechanical properties (ultimate tensile strength and elongation of Hastalex: 2.5, 3.5, and 5-fold ≫ GORE-TEX in the longitudinal direction, transverse direction, and uniform elongation) ↑ Contact angle (both shiny and opaque surface) ↑ Smooth and structured surface ↑ CPAM (2.2 folds than control sample and 7.5 folds than GORE-TEX) ↓ Adherent platelets (2-folds) ↓ Calcium deposits of the connective tissue capsules ↓ Thickness of the fibrous capsule around	2020, 205

For example, in one study, AZ31B Mg alloy surfaces were modified by chitosan-functionalized GO (GOCS) and then immersed in a heparin solution, and five coating layers were fabricated by repeating this cycle five times (Fig. 11).[169] According to the results of electrochemical corrosion tests, GO anti-permeability and negatively charged heparin inhibited the penetration of molecules and ions, providing high corrosion resistance. An analysis of platelet adhesion, cGMP, and hemolysis rate was performed to determine the blood compatibility of the Mg-GOCS/heparin stent. Prior studies showed that fibrinogen adhesion decreased with increasing wettability, which resulted in a reduction in adhered platelets and thrombus formation.[172,173] Therefore, almost no adhered platelets were reported on the Mg-GOCS/heparin stent, since chitosan and GO were proven to be blood compatible and heparin increased the hydrophilicity of the surface. Further, the high level of cGMP expression suggests low platelet activation, and markedly higher cGMP levels were detected in modified samples *versus* unmodified Mg alloy stent samples.[174,175]

If red blood cells are to perform normally when interacting with biomaterials, their hemolysis rate should be below 5%. Nevertheless, a 30% hemolysis rate was observed in the unmodified sample due to its poor corrosion resistance and the production of high amounts of Mg^{2+} and hydrogen peroxide, which resulted in blood cells rupturing and hemolysis.[176] On the other hand, the hemolysis rate of Mg-GOCS/heparin stents

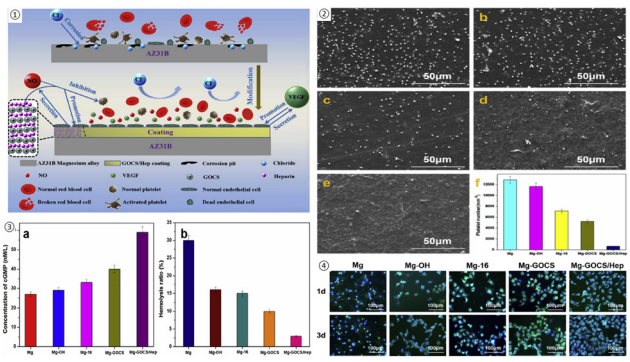

Fig. 11 (1) The schematic of the corrosion resistance mechanism of Mg alloys with GOCS/Hep coating; (2) the SEM image and the number of adhered platelets on different samples ((a) Mg, (b) Mg–OH, (c) Mg-16, (d) Mg-GOCS, (e) Mg-GOCS/Hep); (3) the results of the concentration cGMP expression and hemolysis ratio in samples; (4) fluorescent images of the endothelial cells cultured on the different samples for 1d and 3d (green is the cytoplasm and blue is the nucleus). Reproduced from ref. 169 with permission from [Elsevier], copyright [2020].

decreased significantly to about 3%. The biocompatibility of stents was assessed by cultivating endothelial cells, and Mg-GOCS/heparin stents enhanced cell proliferation significantly with better-spreading morphologies. In addition, modified stents also contain higher levels of VEGF, a highly specific vascular endothelial growth factor, which improves endothelial cell differentiation and maintenance.[177] Lastly, nitric oxide (NO) was measured as an indicator of endothelial cells' health and normal physiological processes.[178,179] A GOCS/heparin coating enhances NO expression, increasing the compatibility of Mg alloy stents since heparin combined with NO reduced platelet activation further and enhanced endothelial cell proliferation.[180,181]

A 3D-printed cardiovascular stent was developed using a hydrogel polymeric composite composed of 2-hydroxyethyl methacrylate (HEMA) and methacrylate GO (MeGO) with loaded resveratrol (RSL).[182] MeGO was found to effectively crosslink the hydrogel, thereby decreasing swelling and maintaining the integrity of the stent. MeGO also provided excellent mechanical properties (the elastic stiffness of the stent was 0.29×10^{-2} MPa (F-ratio = 1.46) and enhanced load-bearing efficiency). There have been numerous studies showing that RSL reduces oxidative stress-induced endothelial apoptosis and increases NO production, preventing platelet adhesion and restoring endothelial function.[175,183,184] According to the RSL release data, the addition of MeGO caused the pores in the structure to be smaller, providing sustained RSL release without initial burst release.[185] The NO release assessment also showed that this stent suppressed platelet adhesion and activation by significantly promoting NO production. In terms of viability results, there was no cytotoxicity observed on HUVECs, and the apoptosis of the cells was reduced up to fivefold.

There are also several vascular diseases that can be treated and revascularized with vascular grafts, including coronary artery disease (CAD), peripheral arterial disease (PAD), abdominal aortic aneurysm (AAA), and aortic dissection (AD).[186] Given autologous blood vessels' limitations, such as their poor quality, non-availability due to patients' diseases, and challenges in surgical interventions and techniques, vascular tissue engineering offers some promising solutions.[187,188] Vascular tissue engineering involves designing and creating artificial blood vessels that can be implanted *in vivo* and provide functional vessels for patients. This can be accomplished with GBM's antibacterial properties and other unique features, which make it perfect for fabricating vascular grafts and alleviating complications after implanting.[19,189] Some of these research results are mentioned in Table 2.

As an example, GO has been used as a coating to promote the mechanical and biological features of decellularized placental and umbilical cord arteries.[187] In vascular grafts, mechanical properties play a key role and should mimic native vessel properties as much as possible; therefore, any mismatch in strain, compliance, and strength or integrity has a significant impact on the success or failure of the implant and the patency rate.[190–192] According to the mechanical evaluation, GO coating did not significantly affect decellularized placental arteries except for its compliance, which increased by 10%. However, GO coating promoted all measured parameters for umbilical cord arteries, including Fmax (the maximum force for rupturing placental and umbilical cord decellularized arteries), burst pressure, strain, and compliance by 27%, 29%, 25%, and 10% respectively. As such, GO coating provides desired mechanical properties with similar values to the native saphenous vein.[193] For both placental and umbilical cord decellularized arteries, platelet adhesion analysis indicated a high value of adhered platelets leading to clot formation. In spite of this, the number of adhered platelets decreased significantly for GO-coated arteries, particularly for umbilical cord arteries. Additionally, antibacterial activity results indicated a drastic reduction of bacterial adhesion (*S. aureus*) for both, which was more pronounced in the placental decellularized arteries. Furthermore, a biological assessment was conducted with human umbilical vein endothelial cells (HUVECs). In accordance with the cytocompatibility results, GO coating not only had no cytotoxic effect on HUVEC adhesion and proliferation, but also, according to previous studies, increased endothelial cell proliferation by forming reactive oxygen and nitrogen species within the cells as well as activating phospho-eNOS and phospho-Akt (Fig. 12).[14,187]

3.3. Graphene in the development of heart valve

Heart valve failure has encompassed a great number of patients suffering from cardiovascular disease.[2] Many attempts have been made to manufacture prosthetic heart valves with the same function and design to treat these kinds of disorders.

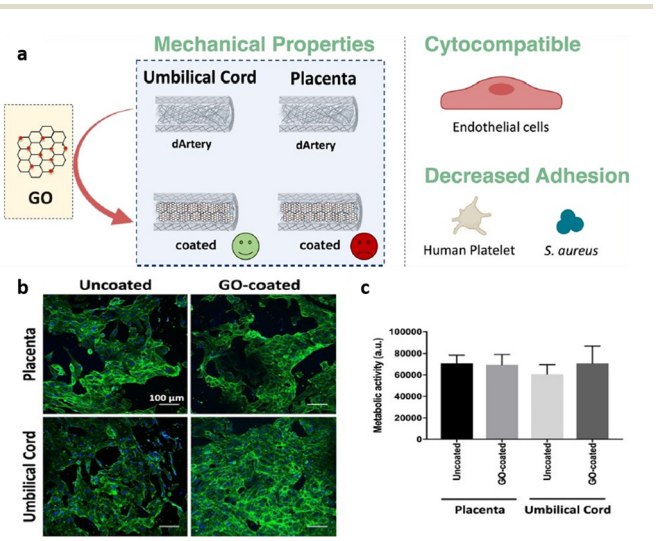

Fig. 12 (a) Schematics of GO coating on decellularized placental and umbilical cord arteries; (b) immunofluorescent images of HUVECs on treated and untreated decellularized placental chorion and umbilical cord arteries HUVECs adherent to uncoated and GO-coated placental chorion and umbilical cord decellularized; (c) the evaluation of metabolic activity of cells by resazurin assay. Reproduced from ref. 187 with permission from [ACS], copyright [2021].

There are three types of heart valve prosthetics: mechanical, biosynthetic valves, and polymeric heart valves.[194–196]

A mechanical valve demonstrates excellent mechanical properties and long-term durability. Nevertheless, due to their geometry and rigid synthetic materials, they increase the risk of thrombosis, requiring patients to take lifelong anticoagulation therapy.[197] Bioprosthetic valves offer better hemodynamic and hemocompatibility than mechanical valves without requiring daily anticoagulants; however, they have some limitations, including leaflet calcification and weak mechanical performance.[198,199] In recent years, polymeric heart valves have been developed to overcome many drawbacks associated with two other types of heart valves by offering a nature-like structure in addition to excellent hemo and biocompatibility. Even so, clinically applying them can still be challenging because of their degradation rate.[200] So far, several research studies have been conducted to develop and improve all types of heart valve prosthetics through various modifications according to Table 2.[201] In terms of biomaterials that can promote the functionality and applicability of heart valve prosthetics in clinics, GBM family members have attracted scientists' attention due to their unique properties for modifying mechanical or bioprosthetic valves, as well as fabricating polymeric valves.

A study, for instance, modified acellular pulmonary valve tissue with rGO as a biosynthetic valve.[1] In the experiment, four groups were defined: poly-L lysine-modified, fibronectin-modified, rGO-modified, and acellular tissue without coating.[1] Platelet activation was studied under dynamic conditions by analyzing markers involved in platelet adhesion and activation, such as CD42a, CD42b, CD41a, CD40, and CD62P. According to the results, there was no significant difference between the rGO-modified sample and the other samples, suggesting that rGO does not activate platelets and can impart thrombo-resistance through rGO. Further, direct contact cytotoxicity results showed 100 g ml^{-1} of rGO significantly reduced L929 fibroblast viability after 24 h. Various studies have reported that cytotoxicity may occur due to disrupted membranes or the formation of reactive oxygen species.[202–204] In the indirect test, however, all samples had approximately 100% viability, and no cytotoxicity was observed. As a result, it can be concluded that rGO does not induce ROS and mechanical damage to the cells' membrane is the main cause of viability reduction in the direct test. By studying DNA fragmentation using TUNEL assays, it was also found that rGO did not cause DNA damage.

A polymeric heart valve is also being developed based on functionalized GO (FGO) and poly(carbonate-urea) urethane known as "Hastalex", whose characteristics have been tested against those of GORE-TEX, a commercial composite for cardiovascular applications.[205] According to the results, Hastalex displayed superior mechanical properties both transversely and longitudinally (3.5-fold and 2.5-fold higher ultimate tensile strength, respectively). Hence, this composite can be more efficient in manufacturing thinner leaflets, as it has higher rigidity and deformability. Regarding biocompatibility, the highest number of viable endothelial cells (Ea.hy 926) exceeded 2.2-fold and 7.5-fold over control and GORE-TEX samples, respectively. The number of adhered platelets in both samples was not significantly different based on the blood platelet adhesion assessment. However, the GORE-TEX surface showed higher platelet deformation than the Hastalex surface. As a result of 60 days of implantation, Hastalex formed a thinner fibrous capsule and was more resistant to calcification, indicating that it is a more biocompatible implant than GORE-TEX.[205]

4. Problems, solutions and future opportunities for GBMs in cardiovascular applications

Questions about the safety of nanoparticles in biomedicine are not new. Despite extensive efforts to understand their safety and toxicity, many questions remain unanswered.[217,218] Similarly, while GBMs possess remarkable properties, concerns persist regarding their biocompatibility and long-term toxicity. The biocompatibility of GBMs may dramatically change by the size, concentration, shape or surface chemistry of the 2D sheet.[219] Many studies have reported conflicting results about the cytotoxic effects of GBMs. If GBMs cannot properly biodegrade, they may accumulate within our bodies.[27] For example, accumulation of GBMs in the heart tissue may trigger an inflammatory response, leading to chronic inflammation and fibrosis.[220] Another potential outcome of GBM accumulation could involve the disruption of the heart's normal electrical activity, given GBMs distinctive properties. Other limitations of GBMs include their potential to interact with cell membranes, leading to membrane damage by forming reactive oxygen species (ROS).[221] Among the cells in our body, red blood cells stand out as particularly sensitive, making them significant considerations for cardiac applications. Red blood cells possess limited repair capabilities and exhibit diminished responsiveness to oxidative stress. Therefore, the premature breakdown of red blood cells (haemolysis) serves as a sensitive indicator of damage induced by GBMs.[222–225] Moreover, several studies have indicated that GO is more prone to inducing thrombosis and platelet activation compared to rGO.[25,226] Research by Singh's group suggests that GO triggers platelet aggregation by activating nonreceptor protein tyrosine kinases of the Src family and releasing intracellular free calcium from cytosolic stores.[227]

Enhancing the biocompatibility of GBMs involves functionalizing their surface; however, it is crucial to consider the long-term stability of these functionalization methods such as surface coatings.[228–230] If the coatings degrade over time, the toxicity may differ significantly from short-term exposure results. Extended studies are necessary to assess whether longer treatment durations influence the nanotoxic potential of GBMs. One strategy that can improve GBM biocompatibility is PEGylation.[231–233] In a study, it was shown that GO may bind to the complement protein C3, which could then be

cleaved, inducing activation of the complement cascade. However, through PEGylation of GO, this process impaired the normal interaction between C3a and its receptor, thereby reducing the adverse complement response to G.[232] PEG has attracted significant attention among various polymeric structures, largely due to its approval by the US Food and Drug Administration (FDA).[234,235] Renowned for its non-toxic, non-immunogenic, and non-antigenic properties, along with its high water solubility, PEGylation effectively reduces reticuloendothelial clearance, extends circulation time, and improves material stability. Current literature indicates that PEGylation decreases the cytotoxicity of various GBMs while enhancing their physiological stability and pharmacokinetic characteristics.[224,236–242] In addition to PEG, various hydrophilic polymers, ranging from natural polymers like dextran to synthetic ones such as polyvinyl alcohol (PVA) and cationic polymers like polyethyleneimine (PEI), polypropyleneimine (PPI), and poly(amidoamine) (PAMAM), have been reported to enhance dispersity and stability and reduce toxicity of GBMs.[25,225,243,244]

Therefore, future research should focus on elucidating the mechanisms underlying GBM-cell interactions and developing strategies to enhance biocompatibility while minimizing toxicity. Furthermore, to enhance the accuracy and comparability of studies, comprehensive physicochemical characterization and standardization are essential in all future investigations concerning the toxicity of GBMs. Experimental descriptions of GBMs should include details such as their size, morphology, surface area, concentration, charge, surface modifications, purity, and agglomeration.[25,163,245–249] The toxicity and biocompatibility of GBMs are largely influenced by these physicochemical factors; therefore, researchers should consider single-factor experimental designs and avoid excluding other interfering parameters. Moreover, conducting various cell experiments in combination with primary cells is essential for cardiac applications, enabling a comprehensive evaluation of the physicochemical properties and toxicity of GBMs.[25,246,247,250] It is essential to investigate the *in vivo* biocompatibility of these nanomaterials through both short-term and long-term studies before utilizing them in biomedical applications.[251–253] Another challenging aspect related to GBMs for cardiac applications is the limited availability of reports on their *in vivo* biocompatibility. Additionally, the majority of existing *in vivo* studies have been conducted in small animals, which presents an additional obstacle.[10,241,245,247,249]

5. Conclusion

Cardiovascular diseases (CVDs) are among the most common health concerns worldwide, so heart transplantation remains the most effective and invasive method of fully recovering heart function.[78] In spite of recent advances in repairing cardiac tissue and restoring its complete function, recent developments have yet to address the unique structural, physical, mechanical, and chemical characteristics of the heart and blood vessels.[8] Many studies have been conducted in order to mimic native-like constructs by applying various types of materials, cells, and fabrication methods.[9] Among several biomaterials to meet this purpose, GBMs may be one of the most promising ones due to their remarkable high electrical, mechanical, and biocompatible properties, as well as their inert chemical properties and compatibility with various fabrication methods that make them an ideal candidate.[4,15,91] This study reviewed the recent applications of GBMs in cardiovascular medicine, including cardiac tissue engineering, vascular grafts, and heart valves. It is expected that GBMs will be used in clinics as effective treatments for cardiovascular diseases, and perhaps will become a great alternative to heart transplants based on the above-mentioned information, despite some serious concerns about their long-term biocompatibility range.

Conflicts of interest

There are no conflicts to declare.

Acknowledgements

We would like to acknowledge the help of Nicholas Seifalian in reading through the table and references for accuracy.

References

1 P. Wilczek, R. Major, L. Lipinska, J. Lackner and A. Mzyk, Thrombogenicity and biocompatibility studies of reduced graphene oxide modified acellular pulmonary valve tissue, *Mater. Sci. Eng., C*, 2015, **53**, 310–321, DOI: **10.1016/j.msec.2015.04.044**.

2 R. A. Rippel, H. Ghanbari and A. M. Seifalian, Tissue-engineered heart valve: future of cardiac surgery, *World J. Surg.*, 2012, **36**, 1581–1591.

3 J. R. Venugopal, M. P. Prabhakaran, S. Mukherjee, R. Ravichandran, K. Dan and S. Ramakrishna, Biomaterial strategies for alleviation of myocardial infarction, *J. R. Soc., Interface*, 2012, **9**(66), 1–19.

4 K. N. Alagarsamy, *et al.*, Carbon nanomaterials for cardiovascular theranostics: Promises and challenges, *Bioact. Mater.*, 2021, **6**(8), 2261–2280, DOI: **10.1016/j.bioactmat.2020.12.030**.

5 X. Yan, H. Sun and P. Yang, Recent Advances on Electroconductive Hydrogels Used in Heart Repair and Regeneration, *Adv. Mater. Sci. Eng.*, 2022, **1**, 6042137, DOI: **10.1155/2022/6042137**.

6 D. Sharma, M. Ferguson, T. J. Kamp and F. Zhao, Constructing biomimetic cardiac tissues: a review of scaffold materials for engineering cardiac patches, *Emergent Mater.*, 2019, **2**(2), 181–191, DOI: **10.1007/s42247-019-00046-4**.

7 Z. Shao, *et al.*, Recent progress in biomaterials for heart valve replacement: Structure, function, and biomimetic design, *View*, 2021, **2**(6), 20200142, DOI: **10.1002/VIW.20200142**.
8 V. Sharma, *et al.*, Recent advances in cardiac tissue engineering for the management of myocardium infarction, *Cells*, 2021, **10**(10), 2538, DOI: **10.3390/cells10102538**.
9 S. Saghebasl, A. Akbarzadeh, A. M. Gorabi, N. Nikzamir, M. SeyedSadjadi and E. Mostafavi, Biodegradable functional macromolecules as promising scaffolds for cardiac tissue engineering, *Polym. Adv. Technol.*, 2022, **33**(7), 2044–2068, DOI: **10.1002/pat.5669**.
10 M. H. Norahan, M. Amroon, R. Ghahremanzadeh, M. Mahmoodi and N. Baheiraei, Electroactive graphene oxide-incorporated collagen assisting vascularization for cardiac tissue engineering, *J. Biomed. Mater. Res., Part A*, 2019, **107**(1), 204–219, DOI: **10.1002/jbm.a.36555**.
11 K. Ashtari, *et al.*, Electrically conductive nanomaterials for cardiac tissue engineering, *Adv. Drug Delivery Rev.*, 2019, **144**, 162–179.
12 M. Tallawi, *et al.*, Strategies for the chemical and biological functionalization of scaffolds for cardiac tissue engineering: a review, *J. R. Soc., Interface*, 2015, **12**(108), 20150254.
13 K. S. Novoselov, V. I. Fal'ko, L. Colombo, P. R. Gellert, M. G. Schwab and K. Kim, A roadmap for graphene, *Nature*, 2012, **490**(7419), 192–200.
14 S. Stankovich, *et al.*, Graphene-based composite materials, *Nature*, 2006, **442**(7100), 282–286.
15 A. Savchenko, R. T. Yin, D. Kireev, I. R. Efimov and E. Molokanova, Graphene-Based Scaffolds: Fundamentals and Applications for Cardiovascular Tissue Engineering, *Front. Bioeng. Biotechnol.*, 2021, **9**, 797340, DOI: **10.3389/fbioe.2021.797340**.
16 R. N. Gomes, *et al.*, Antimicrobial graphene nanoplatelets coatings for silicone catheters, *Carbon*, 2018, **139**, 635–647.
17 A. T. Pereira, *et al.*, Graphene-based materials: The key for the successful application of pHEMA as a blood-contacting device, *Biomater. Sci.*, 2021, **9**(9), 3362–3377.
18 A. T. Pereira, P. C. Henriques, P. C. Costa, M. C. L. Martins, F. D. Magalhaes and I. C. Goncalves, Graphene oxide-reinforced poly (2-hydroxyethyl methacrylate) hydrogels with extreme stiffness and high-strength, *Compos. Sci. Technol.*, 2019, **184**, 107819.
19 P. C. Henriques, I. Borges, A. M. Pinto, F. D. Magalhaes and I. C. Goncalves, Fabrication and antimicrobial performance of surfaces integrating graphene-based materials, *Carbon*, 2018, **132**, 709–732.
20 I. E. P. Souza, L. V. Cambraia, V. S. Gomide and E. H. M. Nunes, Short review on the use of graphene as a biomaterial –prospects, and challenges in Brazil, *J. Mater. Res. Technol.*, 2022, **19**, 2410–2430, DOI: **10.1016/j.jmrt.2022.05.170**.
21 N. Amiryaghoubi and M. Fathi, Bioscaffolds of graphene based-polymeric hybrid materials for myocardial tissue engineering, *BioImpacts*, 2024, **14**(1), DOI: **10.34172/bi.2023.27684**.
22 W.-W. Liu, S.-P. Chai, A. R. Mohamed and U. Hashim, Synthesis and characterization of graphene and carbon nanotubes: A review on the past and recent developments, *J. Ind. Eng. Chem.*, 2014, **20**(4), 1171–1185, DOI: **10.1016/j.jiec.2013.08.028**.
23 Y. M. Manawi, Ihsanullah, A. Samara, T. Al-Ansari and M. A. Atieh, A review of carbon nanomaterials' synthesis via the chemical vapor deposition (CVD) method, *Materials*, 2018, **11**(5), 822, DOI: **10.3390/ma11050822**.
24 J.-H. Lee, S.-J. Park and J.-W. Choi, Electrical property of graphene and its application to electrochemical biosensing, *Nanomaterials*, 2019, **9**(2), 297.
25 Y. Xiao, *et al.*, Synthesis and functionalization of graphene materials for biomedical applications: recent advances, challenges, and perspectives, *Adv. Sci.*, 2023, **10**(9), 2205292.
26 J. Li, H. Zeng, Z. Zeng, Y. Zeng and T. Xie, Promising graphene-based nanomaterials and their biomedical applications and potential risks: A comprehensive review, *ACS Biomater. Sci. Eng.*, 2021, **7**(12), 5363–5396.
27 P. Zare, M. Aleemardani, A. Seifalian, Z. Bagher and A. M. Seifalian, Graphene Oxide: Opportunities and Challenges in Biomedicine, *Nanomaterials*, 2021, **11**(5), 1083.
28 L. Yao, A. Chen, L. Li and Y. Liu, Preparation, properties, applications and outlook of graphene-based materials in biomedical field: a comprehensive review, *J. Biomater. Sci., Polym. Ed.*, 2023, **34**(8), 1121–1156.
29 F. Kuang, T. Hui, Y. Chen, M. Qiu and X. Gao, Post–Graphene 2D Materials: Structures, Properties, and Cancer Therapy Applications, *Adv. Healthc. Mater.*, 2024, **13**(5), 2302604.
30 M. Aleemardani, P. Zare, A. Seifalian, Z. Bagher and A. M. Seifalian, Graphene-based materials prove to be a promising candidate for nerve regeneration following peripheral nerve injury, *Biomedicines*, 2021, **10**(1), 73.
31 P. Zare, M. Aleemardani, A. Seifalian, Z. Bagher and A. M. Seifalian, Graphene oxide: Opportunities and challenges in biomedicine, *Nanomaterials*, 2021, **11**(5), 1083.
32 M. Sekuła-Stryjewska, *et al.*, Graphene-based materials enhance cardiomyogenic and angiogenic differentiation capacity of human mesenchymal stem cells in vitro – Focus on cardiac tissue regeneration, *Mater. Sci. Eng., C*, 2021, **119**, 111614, DOI: **10.1016/j.msec.2020.111614**.
33 F. Edrisi, N. Baheiraei, M. Razavi, K. Roshanbinfar, R. Imani and N. Jalilinejad, Potential of graphene-based nanomaterials for cardiac tissue engineering, *J. Mater. Chem. B*, 2023, **11**(31), 7280–7299, DOI: **10.1039/D3TB00654A**.
34 H. Jawad, N. N. Ali, A. R. Lyon, Q. Z. Chen, S. E. Harding and A. R. Boccaccini, Myocardial tissue engineering: a review, *J. Tissue Eng. Regener. Med.*, 2007, **1**(5), 327–342.
35 Q.-Z. Chen, S. E. Harding, N. N. Ali, A. R. Lyon and A. R. Boccaccini, Biomaterials in cardiac tissue engineer-

ing: ten years of research survey, *Mater. Sci. Eng., R*, 2008, **59**(1–6), 1–37.
36 C. Lee, X. Wei, J. W. Kysar and J. Hone, Measurement of the elastic properties and intrinsic strength of monolayer graphene, *Science*, 2008, **321**(5887), 385–388.
37 R. Geetha Bai, N. Ninan, K. Muthoosamy and S. Manickam, Graphene: A versatile platform for nanotheranostics and tissue engineering, *Prog. Mater. Sci.*, 2018, **91**, 24–69, DOI: **10.1016/j.pmatsci.2017.08.004**.
38 G. Reina, J. M. González-Domínguez, A. Criado, E. Vázquez, A. Bianco and M. Prato, Promises, facts and challenges for graphene in biomedical applications, *Chem. Soc. Rev.*, 2017, **46**(15), 4400–4416, DOI: **10.1039/c7cs00363c**.
39 D. W. Johnson, B. P. Dobson and K. S. Coleman, A manufacturing perspective on graphene dispersions, *Curr. Opin. Colloid Interface Sci.*, 2015, **20**(5–6), 367–382.
40 Y. Xiao, *et al.*, Synthesis and Functionalization of Graphene Materials for Biomedical Applications: Recent Advances, Challenges, and Perspectives, *Adv. Sci.*, 2023, **10**(9), 2205292, DOI: **10.1002/advs.202205292**.
41 C. N. R. Rao, *et al.*, A study of the synthetic methods and properties of graphenes, *Sci. Technol. Adv. Mater.*, 2010, **11**(5), 054502.
42 X. Wang, Y. Wei, H. Zhou, Q. Liu and L. Zhu, Synthesis of graphene nanosheets by the electrical explosion of graphite powder confined in a tube, *Ceram. Int.*, 2021, **47**(15), 21934–21942.
43 J. Chen, *et al.*, One-step reduction and PEGylation of graphene oxide for photothermally controlled drug delivery, *Biomaterials*, 2014, **35**(18), 4986–4995.
44 Y. Qu, *et al.*, Advances on graphene-based nanomaterials for biomedical applications, *Mater. Sci. Eng., C*, 2018, **90**, 764–780, DOI: **10.1016/j.msec.2018.05.018**.
45 V. C. Scanlon and T. Sanders, *Essentials of anatomy and physiology*, FA Davis, 2018.
46 R. Bao, B. Tan, S. Liang, N. Zhang, W. Wang and W. Liu, A π–π conjugation-containing soft and conductive injectable polymer hydrogel highly efficiently rebuilds cardiac function after myocardial infarction, *Biomaterials*, 2017, **122**, 63–71, DOI: **10.1016/j.biomaterials.2017.01.012**.
47 T. Doenst, T. D. Nguyen and E. D. Abel, Cardiac metabolism in heart failure: implications beyond ATP production, *Circ. Res.*, 2013, **113**(6), 709–724.
48 M. Solazzo, F. J. O'Brien, V. Nicolosi and M. G. Monaghan, The rationale and emergence of electroconductive biomaterial scaffolds in cardiac tissue engineering, *APL Bioeng.*, 2019, **3**(4), DOI: **10.1063/1.5116579**.
49 A. Ul Haq, *et al.*, Extrinsically conductive nanomaterials for cardiac tissue engineering applications, *Micromachines*, 2021, **12 (8)**, 914, DOI: **10.3390/mi12080914**.
50 X. Wu, S. J. Ding, K. Lin and J. Su, A review on the biocompatibility and potential applications of graphene in inducing cell differentiation and tissue regeneration, *J. Mater. Chem. B*, 2017, **5**(17), 3084–3102, DOI: **10.1039/c6tb03067j**.
51 J. Arkowski, M. Obremska, K. Kędzierski, A. Sławuta and M. Wawrzyńska, Applications for graphene and its derivatives in medical devices: Current knowledge and future applications, *Adv. Clin. Exp. Med.*, 2021, **29**(12), 1497–1504, DOI: **10.17219/ACEM/130601**.
52 J. Kailashiya, N. Singh, S. K. Singh, V. Agrawal and D. Dash, Graphene oxide-based biosensor for detection of platelet-derived microparticles: a potential tool for thrombus risk identification, *Biosens. Bioelectron.*, 2015, **65**, 274–280.
53 P. Kalluru, R. Vankayala, C.-S. Chiang and K. C. Hwang, Nano-graphene oxide-mediated In vivo fluorescence imaging and bimodal photodynamic and photothermal destruction of tumors, *Biomaterials*, 2016, **95**, 1–10.
54 Z. Fan, *et al.*, Near-infrared light-triggered unfolding microneedle patch for minimally invasive treatment of myocardial ischemia, *ACS Appl. Mater. Interfaces*, 2021, **13**(34), 40278–40289.
55 F. Perreault, A. F. De Faria, S. Nejati and M. Elimelech, Antimicrobial properties of graphene oxide nanosheets: why size matters, *ACS Nano*, 2015, **9**(7), 7226–7236.
56 O. Akhavan and E. Ghaderi, Toxicity of graphene and graphene oxide nanowalls against bacteria, *ACS Nano*, 2010, **4**(10), 5731–5736.
57 J. Wang, Y. Wei, X. Shi and H. Gao, Cellular entry of graphene nanosheets: the role of thickness, oxidation and surface adsorption, *RSC Adv.*, 2013, **3**(36), 15776–15782.
58 Y. Tu, *et al.*, Destructive extraction of phospholipids from Escherichia coli membranes by graphene nanosheets, *Nat. Nanotechnol.*, 2013, **8**(8), 594–601.
59 S. Ullah, *et al.*, Tobramycin mediated silver nanospheres/graphene oxide composite for synergistic therapy of bacterial infection, *J. Photochem. Photobiol., B*, 2018, **183**, 342–348.
60 J. Han, *et al.*, Dual roles of graphene oxide to attenuate inflammation and elicit timely polarization of macrophage phenotypes for cardiac repair, *ACS Nano*, 2018, **12**(2), 1959–1977.
61 G. Choe, *et al.*, Anti-oxidant activity reinforced reduced graphene oxide/alginate microgels: mesenchymal stem cell encapsulation and regeneration of infarcted hearts, *Biomaterials*, 2019, **225**, 119513.
62 A. M. Pinto, *et al.*, Smaller particle size and higher oxidation improves biocompatibility of graphene-based materials, *Carbon*, 2016, **99**, 318–329.
63 M. Orecchioni, D. Bedognetti, F. Sgarrella, F. M. Marincola, A. Bianco and L. G. Delogu, Impact of carbon nanotubes and graphene on immune cells, *J. Transl. Med.*, 2014, **12**, 1–11.
64 S. P. Mukherjee, *et al.*, Next–Generation Sequencing Reveals Differential Responses to Acute versus Long–Term Exposures to Graphene Oxide in Human Lung Cells, *Small*, 2020, **16**(21), 1907686.
65 G. Duan, *et al.*, Protein corona mitigates the cytotoxicity of graphene oxide by reducing its physical interaction with cell membrane, *Nanoscale*, 2015, **7**(37), 15214–15224.

66 Y. Li, *et al.*, The triggering of apoptosis in macrophages by pristine graphene through the MAPK and TGF-beta signaling pathways, *Biomaterials*, 2012, **33**(2), 402–411.
67 E. Demirel, E. Karaca and Y. Y. Durmaz, Effective PEGylation method to improve biocompatibility of graphene derivatives, *Eur. Polym. J.*, 2020, **124**, 109504.
68 Y. Li, *et al.*, Surface coating–dependent cytotoxicity and degradation of graphene derivatives: Towards the design of non–toxic, degradable nano–graphene, *Small*, 2014, **10**(8), 1544–1554.
69 K. Yang, Y. Li, X. Tan, R. Peng and Z. Liu, Behavior and toxicity of graphene and its functionalized derivatives in biological systems, *Small*, 2013, **9**(9–10), 1492–1503.
70 J. Li, H. Zeng, Z. Zeng, Y. Zeng and T. Xie, Promising Graphene-Based Nanomaterials and Their Biomedical Applications and Potential Risks: A Comprehensive Review, *ACS Biomater. Sci. Eng.*, 2021, **7**(12), 5363–5396, DOI: **10.1021/acsbiomaterials.1c00875**.
71 J. Park, *et al.*, Graphene potentiates the myocardial repair efficacy of mesenchymal stem cells by stimulating the expression of angiogenic growth factors and gap junction protein, *Adv. Funct. Mater.*, 2015, **25**(17), 2590–2600.
72 A. K. Barui, A. Roy, S. Das, K. Bhamidipati and C. R. Patra, Therapeutic applications of graphene oxides in angiogenesis and cancers, *Nanoparticles and their biomedical applications*, 2020, pp. 147–189.
73 M. Sekuła-Stryjewska, *et al.*, Graphene-based materials enhance cardiomyogenic and angiogenic differentiation capacity of human mesenchymal stem cells in vitro–focus on cardiac tissue regeneration, *Mater. Sci. Eng., C*, 2021, **119**, 111614.
74 S. Mukherjee, *et al.*, Graphene oxides show angiogenic properties, *Adv. Healthc. Mater.*, 2015, **4**(11), 1722–1732.
75 E. Chavakis and S. Dimmeler, Regulation of endothelial cell survival and apoptosis during angiogenesis, *Arterioscler., Thromb., Vasc. Biol.*, 2002, **22**(6), 887–893.
76 F. Weinberger, I. Mannhardt and T. Eschenhagen, Engineering cardiac muscle tissue: a maturating field of research, *Circ. Res.*, 2017, **120**(9), 1487–1500.
77 N. Kiaie, A. M. Gorabi, S. H. Ahmadi Tafti and S. Rabbani, Pre-vascularization Approaches for Heart Tissue Engineering, *Regener. Eng. Transl. Med.*, 2021, **7**(4), 450–459, DOI: **10.1007/s40883-020-00172-0**.
78 M. D. Dozois, L. C. Bahlmann, Y. Zilberman and X. (Shirley) Tang, Carbon nanomaterial-enhanced scaffolds for the creation of cardiac tissue constructs: A new frontier in cardiac tissue engineering, *Carbon*, 2017, **120**, 338–349, DOI: **10.1016/j.carbon.2017.05.050**.
79 H. M. El-Husseiny, E. A. Mady, W. A. El-Dakroury, A. S. Doghish and R. Tanaka, Stimuli-responsive hydrogels: smart state of-the-art platforms for cardiac tissue engineering, *Front. Bioeng. Biotechnol.*, 2023, **11**, 1174075, DOI: **10.3389/fbioe.2023.1174075**.
80 S. R. Shin, *et al.*, Carbon-nanotube-embedded hydrogel sheets for engineering cardiac constructs and bioactuators, *ACS Nano*, 2013, **7**(3), 2369–2380.
81 Y. Wu, L. Wang, B. Guo and P. X. Ma, Interwoven aligned conductive nanofiber yarn/hydrogel composite scaffolds for engineered 3D cardiac anisotropy, *ACS Nano*, 2017, **11**(6), 5646–5659.
82 M. Maleki, *et al.*, Graphene Oxide: A Promising Material for Regenerative Medicine and Tissue Engineering, *Biomol. Concepts*, 2021, **11**(1), 182–200, DOI: **10.1515/bmc-2020-0017**.
83 P. Memarian, A. Solouk, Z. Bagher, S. Akbari and M. H. Nazarpak, Ionic conductive nanocomposite based on poly (l-lactic acid)/poly (amidoamine) dendrimerelectrospun nanofibrous for biomedical application, *Biomed. Mater.*, 2021, **17**(1), 015007.
84 O. Lozano, A. Torres-Quintanilla and G. García-Rivas, Nanomedicine for the cardiac myocyte: where are we?, *J. Controlled Release*, 2018, **271**, 149–165.
85 M. Farokhi, M. Aleemardani, A. Solouk, H. Mirzadeh, A. H. Teuschl and H. Redl, Crosslinking strategies for silk fibroin hydrogels: Promising biomedical materials, *Biomed. Mater.*, 2021, **16**(2), 022004.
86 S. K. Jaganathan, E. Supriyanto, S. Murugesan, A. Balaji and M. K. Asokan, Biomaterials in cardiovascular research: applications and clinical implications, *BioMed Res. Int.*, 2014, **1**, 459465, DOI: **10.1155/2014/459465**.
87 L. Vogt, F. Ruther, S. Salehi and A. R. Boccaccini, Poly (glycerol sebacate) in biomedical applications—A review of the recent literature, *Adv. Healthc. Mater.*, 2021, **10**(9), 2002026.
88 M. Azizi, M. Navidbakhsh, S. Hosseinzadeh and M. Sajjadi, Cardiac cell differentiation of muscle satellite cells on aligned composite electrospun polyurethane with reduced graphene oxide, *J. Polym. Res.*, 2019, **26**(11), 1–9, DOI: **10.1007/s10965-019-1936-9**.
89 J. Zhou, *et al.*, Injectable OPF/graphene oxide hydrogels provide mechanical support and enhance cell electrical signaling after implantation into myocardial infarct, *Theranostics*, 2018, **8**(12), 3317–3330, DOI: **10.7150/thno.25504**.
90 M. Kavousi Heidari, *et al.*, Wound dressing based on PVA nanofiber containing silk fibroin modified with GO/ZnO nanoparticles for superficial wound healing: In vitro and in vivo evaluations, *Biotechnol. Prog.*, 2023, **39**(3), e3331, DOI: **10.1002/btpr.3331**.
91 W. Xue, *et al.*, Preparation, Properties, and Application of Graphene-Based Materials in Tissue Engineering Scaffolds, *Tissue Eng., Part B*, 2022, **28**(5), 1121–1136, DOI: **10.1089/ten.teb.2021.0127**.
92 S. Tiwari, R. Patil, S. K. Dubey and P. Bahadur, Graphene nanosheets as reinforcement and cell-instructive material in soft tissue scaffolds, *Adv. Colloid Interface Sci.*, 2020, **281**, 102167.
93 X. Chen, *et al.*, Characteristics and toxicity assessment of electrospun gelatin/PCL nanofibrous scaffold loaded with graphene in vitro and in vivo, *Int. J. Nanomed.*, 2019, **14**, 3669–3678, DOI: **10.2147/IJN.S204971**.

94 S. Bahrami, *et al.*, Three-dimensional graphene foam as a conductive scaffold for cardiac tissue engineering, *J. Biomater. Appl.*, 2019, **34**(1), 74–85, DOI: **10.1177/0885328219839037**.

95 A. Ghofrani, L. Taghavi, B. Khalilivavdareh, A. Rohani Shirvan and A. Nouri, Additive manufacturing and advanced functionalities of cardiac patches: A review, *Eur. Polym. J.*, 2022, **174**, 111332, DOI: **10.1016/j.eurpolymj.2022.111332**.

96 H. P. Ferreira, *et al.*, Using Graphene-Based Materials for Stiff and Strong Poly(ethylene glycol) Hydrogels, *Int. J. Mol. Sci.*, 2022, **23**(4), 2312, DOI: **10.3390/ijms23042312**.

97 J. L. Ifkovits, *et al.*, Injectable hydrogel properties influence infarct expansion and extent of postinfarction left ventricular remodeling in an ovine model, *Proc. Natl. Acad. Sci. U. S. A.*, 2010, **107**(25), 11507–11512.

98 N. Karimi Hajishoreh, N. Baheiraei, N. Naderi, M. Salehnia and M. Razavi, Left Ventricular Geometry and Angiogenesis Improvement in Rat Chronic Ischemic Cardiomyopathy following Injection of Encapsulated Mesenchymal Stem Cells, *Cell J.*, 2022, **24**(12), 741–747, DOI: **10.22074/CELLJ.2022.557257.1040**.

99 S. R. Shin, *et al.*, Reduced graphene oxide–gelMA hybrid hydrogels as scaffolds for cardiac tissue engineering, *Small*, 2016, **12**(27), 3677–3689.

100 G. Zhao, *et al.*, Anisotropic conductive reduced graphene oxide/silk matrices promote post-infarction myocardial function by restoring electrical integrity, *Acta Biomater.*, 2022, **139**, 190–203, DOI: **10.1016/j.actbio.2021.03.073**.

101 S. Saravanan, *et al.*, Graphene Oxide-Gold Nanosheets Containing Chitosan Scaffold Improves Ventricular Contractility and Function After Implantation into Infarcted Heart, *Sci. Rep.*, 2018, **8**(1), 15069, DOI: **10.1038/s41598-018-33144-0**.

102 V. Martinelli, *et al.*, Carbon nanotubes promote growth and spontaneous electrical activity in cultured cardiac myocytes, *Nano Lett.*, 2012, **12**(4), 1831–1838.

103 B. D. Ratner, The catastrophe revisited: blood compatibility in the 21st century, *Biomaterials*, 2007, **28**(34), 5144–5147.

104 B. D. Ratner, A. S. Hoffman, F. J. Schoen and J. E. Lemons, *Biomaterials science: an introduction to materials in medicine*, Elsevier, 2004.

105 Y. Shapira, M. Vaturi and A. Sagie, Hemolysis associated with prosthetic heart valves: a review, *Cardiol. Rev.*, 2009, **17**(3), 121–124.

106 A. Sasidharan, *et al.*, Hemocompatibility and macrophage response of pristine and functionalized graphene, *Small*, 2012, **8**(8), 1251–1263.

107 R. N. Urankar, *et al.*, Expansion of cardiac ischemia/reperfusion injury after instillation of three forms of multi-walled carbon nanotubes, *Part. Fibre Toxicol.*, 2012, **9**, 1–16.

108 H. B. Bostan, *et al.*, Cardiotoxicity of nano-particles, *Life Sci.*, 2016, **165**, 91–99.

109 R. K. Roy, *et al.*, Hemocompatibility of surface-modified, silicon-incorporated, diamond-like carbon films, *Acta Biomater.*, 2009, **5**(1), 249–256.

110 J. F. Hecker and L. A. Scandrett, Roughness and thrombogenicity of the outer surfaces of intravascular catheters, *J. Biomed. Mater. Res.*, 1985, **19**(4), 381–395.

111 M. I. Jones, I. R. McColl, D. M. Grant, K. G. Parker and T. L. Parker, Protein adsorption and platelet attachment and activation, on TiN, TiC, and DLC coatings on titanium for cardiovascular applications, *J. Biomed. Mater. Res.*, 2000, **52**(2), 413–421.

112 T. Hasebe, *et al.*, Effects of surface roughness on antithrombogenicity of diamond-like carbon films, *Diamond Relat. Mater.*, 2007, **16**(4–7), 1343–1348.

113 X. Meng, *et al.*, Enhanced Hemocompatibility of a Direct Chemical Vapor Deposition-Derived Graphene Film, *ACS Appl. Mater. Interfaces*, 2021, **13**(4), 4835–4843, DOI: **10.1021/acsami.0c19790**.

114 J. Kayat, V. Gajbhiye, R. K. Tekade and N. K. Jain, Pulmonary toxicity of carbon nanotubes: a systematic report, *Nanomedicine*, 2011, **7**(1), 40–49.

115 P. A. Stapleton, *et al.*, Impairment of coronary arteriolar endothelium-dependent dilation after multi-walled carbon nanotube inhalation: a time-course study, *Int. J. Mol. Sci.*, 2012, **13**(11), 13781–13803.

116 S. Murugesan, S. A. Mousa, L. J. O'Connor, D. W. Lincoln II and R. J. Linhardt, Carbon inhibits vascular endothelial growth factor-and fibroblast growth factor-promoted angiogenesis, *FEBS Lett.*, 2007, **581**(6), 1157–1160.

117 S. Kanakia, *et al.*, Dose ranging, expanded acute toxicity and safety pharmacology studies for intravenously administered functionalized graphene nanoparticle formulations, *Biomaterials*, 2014, **35**(25), 7022–7031.

118 H. Fan, *et al.*, Fabrication, mechanical properties, and biocompatibility of graphene-reinforced chitosan composites, *Biomacromolecules*, 2010, **11**(9), 2345–2351.

119 V. Georgakilas, *et al.*, Functionalization of graphene: covalent and non-covalent approaches, derivatives and applications, *Chem. Rev.*, 2012, **112**(11), 6156–6214.

120 L. Zhang, Z. Lu, Q. Zhao, J. Huang, H. Shen and Z. Zhang, Enhanced chemotherapy efficacy by sequential delivery of siRNA and anticancer drugs using PEI–grafted graphene oxide, *Small*, 2011, **7**(4), 460–464.

121 H. Kim, R. Namgung, K. Singha, I.-K. Oh and W. J. Kim, Graphene oxide–polyethylenimine nanoconstruct as a gene delivery vector and bioimaging tool, *Bioconjugate Chem.*, 2011, **22**(12), 2558–2567.

122 H. Zare-Zardini, A. Taheri-Kafrani, M. Ordooei, A. Amiri and M. Karimi-Zarchi, Evaluation of toxicity of functionalized graphene oxide with ginsenoside Rh2, lysine and arginine on blood cancer cells (K562), red blood cells, blood coagulation and cardiovascular tissue: In vitro and in vivo studies, *J. Taiwan Inst. Chem. Eng.*, 2018, **93**, 70–78, DOI: **10.1016/j.jtice.2018.08.010**.

123 K.-H. Liao, Y.-S. Lin, C. W. Macosko and C. L. Haynes, Cytotoxicity of graphene oxide and graphene in human

erythrocytes and skin fibroblasts, *ACS Appl. Mater. Interfaces*, 2011, **3**(7), 2607–2615.
124 A. Lakoma and E. S. Kim, Minimally invasive surgical management of benign breast lesions, *Gland Surg.*, 2014, **3**(2), 142.
125 L. G. Svensson, *et al.*, Minimally invasive versus conventional mitral valve surgery: a propensity-matched comparison, *J. Thorac. Cardiovasc. Surg.*, 2010, **139**(4), 926–932.
126 T. Li, Y. Li, X. Wang, X. Li and J. Sun, Thermally and near-infrared light-induced shape memory polymers capable of healing mechanical damage and fatigued shape memory function, *ACS Appl. Mater. Interfaces*, 2019, **11**(9), 9470–9477.
127 W. Xiong, *et al.*, A Vascularized Conductive Elastic Patch for the Repair of Infarcted Myocardium through Functional Vascular Anastomoses and Electrical Integration, *Adv. Funct. Mater.*, 2022, **32**(19), 2111273.
128 C. Hirschhäuser, *et al.*, Connexin 43 phosphorylation by casein kinase 1 is essential for the cardioprotection by ischemic preconditioning, *Basic Res. Cardiol.*, 2021, **116**, 1–18.
129 S. Chakraborty, T. Ponrasu, S. Chandel, M. Dixit and V. Muthuvijayan, Reduced graphene oxide-loaded nanocomposite scaffolds for enhancing angiogenesis in tissue engineering applications, *R. Soc. Open Sci.*, 2018, **5**(5), 172017, DOI: **10.1098/rsos.172017**.
130 H. Bae, *et al.*, Building vascular networks, *Sci. Transl. Med.*, 2012, **4**(160), 160ps23.
131 M. Lovett, K. Lee, A. Edwards and D. L. Kaplan, Vascularization strategies for tissue engineering, *Tissue Eng., Part B*, 2009, **15**(3), 353–370.
132 F. Edrisi, N. Baheiraei, M. Razavi, K. Roshanbinfar, R. Imani and N. Jalilinejad, Potential of graphene-based nanomaterials for cardiac tissue engineering, *J. Mater. Chem. B*, 2023, **11**, 7280–7299, DOI: **10.1039/D3TB00654A**.
133 M. Sekuła-Stryjewska, *et al.*, Graphene-based materials enhance cardiomyogenic and angiogenic differentiation capacity of human mesenchymal stem cells in vitro – Focus on cardiac tissue regeneration, *Mater. Sci. Eng., C*, 2021, **119**, 111614, DOI: **10.1016/j.msec.2020.111614**.
134 M. Heil, I. Eitenmüller, T. Schmitz-Rixen and W. Schaper, Arteriogenesis versus angiogenesis: similarities and differences, *J. Cell. Mol. Med.*, 2006, **10**(1), 45–55.
135 L. Jiang, *et al.*, Preparation of an Electrically Conductive Graphene Oxide/Chitosan Scaffold for Cardiac Tissue Engineering, *Appl. Biochem. Biotechnol.*, 2019, **188**(4), 952–964, DOI: **10.1007/s12010-019-02967-6**.
136 A. Paul, *et al.*, Injectable graphene oxide/hydrogel-based angiogenic gene delivery system for vasculogenesis and cardiac repair, *ACS Nano*, 2014, **8**(8), 8050–8062.
137 H. Sun, *et al.*, Carbon nanotubes enhance intercalated disc assembly in cardiac myocytes via the β1-integrin-mediated signaling pathway, *Biomaterials*, 2015, **55**, 84–95.
138 A. Bianco, Graphene: safe or toxic? The two faces of the medal, *Angew. Chem., Int. Ed.*, 2013, **52**(19), 4986–4997.
139 J. Saleem, L. Wang and C. Chen, Carbon-Based Nanomaterials for Cancer Therapy via Targeting Tumor Microenvironment, *Adv. Healthcare Mater.*, 2018, **7**(20), 1800525, DOI: **10.1002/adhm.201800525**.
140 D. Yang, *et al.*, In vivo targeting of metastatic breast cancer via tumor vasculature-specific nano-graphene oxide, *Biomaterials*, 2016, **104**, 361–371.
141 P. X. Lai, *et al.*, Ultrastrong trapping of VEGF by graphene oxide: Anti-angiogenesis application, *Biomaterials*, 2016, **109**, 12–22, DOI: **10.1016/j.biomaterials.2016.09.005**.
142 J. Müller-Ehmsen, *et al.*, Survival and development of neonatal rat cardiomyocytes transplanted into adult myocardium, *J. Mol. Cell Cardiol.*, 2002, **34**(2), 107–116.
143 G. Choe, *et al.*, Anti-oxidant activity reinforced reduced graphene oxide/alginate microgels: mesenchymal stem cell encapsulation and regeneration of infarcted hearts, *Biomaterials*, 2019, **225**, 119513.
144 J. Müller-Ehmsen, *et al.*, Effective engraftment but poor mid-term persistence of mononuclear and mesenchymal bone marrow cells in acute and chronic rat myocardial infarction, *J. Mol. Cell Cardiol.*, 2006, **41**(5), 876–884.
145 D. M. Nelson, Z. Ma, K. L. Fujimoto, R. Hashizume and W. R. Wagner, Intra-myocardial biomaterial injection therapy in the treatment of heart failure: Materials, outcomes and challenges, *Acta Biomater.*, 2011, **7**(1), 1–15.
146 H. Zhang, *et al.*, Injection of bone marrow mesenchymal stem cells in the borderline area of infarcted myocardium: heart status and cell distribution, *J. Thorac. Cardiovasc. Surg.*, 2007, **134**(5), 1234–1240.
147 R. Lakshmanan and N. Maulik, Development of next generation cardiovascular therapeutics through bio-assisted nanotechnology, *J. Biomed. Mater. Res., Part B*, 2018, **106**(5), 2072–2083, DOI: **10.1002/jbm.b.34000**.
148 R. S. Mahla, Stem cells applications in regenerative medicine and disease therapeutics, *Int. J. Cell Biol.*, 2016, **1**, 6940283, DOI: **10.1155/2016/6940283**.
149 H. Arzaghi, *et al.*, Nanomaterials modulating stem cell behavior towards cardiovascular cell lineage, *Mater. Adv.*, 2021, **2**(7), 2231–2262, DOI: **10.1039/d0ma00957a**.
150 N. Karimi Hajishoreh, N. Baheiraei, N. Naderi and M. Salehnia, Reduced graphene oxide facilitates biocompatibility of alginate for cardiac repair, *J. Bioact. Compat. Polym.*, 2020, **35**(4–5), 363–377, DOI: **10.1177/0883911520933913**.
151 J. Park, *et al.*, Graphene-regulated cardiomyogenic differentiation process of mesenchymal stem cells by enhancing the expression of extracellular matrix proteins and cell signaling molecules, *Adv. Healthc. Mater.*, 2014, **3**(2), 176–181.
152 E. Bressan, *et al.*, Graphene based scaffolds effects on stem cells commitment, *J. Transl. Med.*, 2014, **12**(1), 1–15.
153 A. J. Ryan, *et al.*, Electroconductive Biohybrid Collagen/Pristine Graphene Composite Biomaterials with Enhanced Biological Activity, *Adv. Mater.*, 2018, **30**(15), 1706442, DOI: **10.1002/adma.201706442**.

154 A. Najafi Tireh Shabankareh, H. Ghanbari and P. Samadi Pakchin, Development of a New Electroconductive Nanofibrous Cardiac Patch Based on Polyurethane-Reduced Graphene Oxide Nanocomposite Scaffolds, 2023, DOI: 10.2139/ssrn.4339940.
155 M. Shi, *et al.*, Micropatterned conductive elastomer patch based on poly (glycerol sebacate)-graphene for cardiac tissue repair, *Biofabrication*, 2022, **14**(3), 035001, DOI: 10.1088/1758-5090/ac59f2.
156 S. Soltani, *et al.*, Development of an Injectable Shear-Thinning Nanocomposite Hydrogel for Cardiac Tissue Engineering, *Gels*, 2022, **8**(2), 121, DOI: 10.3390/gels8020121.
157 Y. Wang, *et al.*, 4D Printed Cardiac Construct with Aligned Myofibers and Adjustable Curvature for Myocardial Regeneration, *ACS Appl. Mater. Interfaces*, 2021, **13**(11), 12746–12758, DOI: 10.1021/acsami.0c17610.
158 A. Fakhrali, *et al.*, Biocompatible graphene–embedded PCL/PGS–based nanofibrous scaffolds: A potential application for cardiac tissue regeneration, *J. Appl. Polym. Sci.*, 2021, **138**(40), 51177.
159 L. Zhang, *et al.*, Biocompatibility and Angiogenic Effect of Chitosan/Graphene Oxide Hydrogel Scaffolds on EPCs, *Stem Cells Int.*, 2021, **1**, 5594370, DOI: 10.1155/2021/5594370.
160 A. Mousavi, S. Mashayekhan, N. Baheiraei and A. Pourjavadi, Biohybrid oxidized alginate/myocardial extracellular matrix injectable hydrogels with improved electromechanical properties for cardiac tissue engineering, *Int. J. Biol. Macromol.*, 2021, **180**, 692–708, DOI: 10.1016/j.ijbiomac.2021.03.097.
161 A. Talebi, S. Labbaf, F. Karimzadeh, E. Masaeli and M.-H. N. Esfahani, Electroconductive graphene-containing polymeric patch: a promising platform for future cardiac repair, *ACS Biomater. Sci. Eng.*, 2020, **6**(7), 4214–4224.
162 Z. Yuan, Q. Qin, M. Yuan, H. Wang and R. Li, Development and novel design of clustery graphene oxide formed Conductive Silk hydrogel cell vesicle to repair and routine care of myocardial infarction: Investigation of its biological activity for cell delivery applications, *J. Drug Delivery Sci. Technol.*, 2020, **60**, 102001, DOI: 10.1016/j.jddst.2020.102001.
163 M. H. Norahan, M. Pourmokhtari, M. R. Saeb, B. Bakhshi, M. S. Zomorrod and N. Baheiraei, Electroactive cardiac patch containing reduced graphene oxide with potential antibacterial properties, *Mater. Sci. Eng., C*, 2019, **104**, 109921.
164 A. Ghasemi, R. Imani, M. Yousefzadeh, S. Bonakdar, A. Solouk and H. Fakhrzadeh, Studying the potential application of electrospun polyethylene terephthalate/graphene oxide nanofibers as electroconductive cardiac patch, *Macromol. Mater. Eng.*, 2019, **304**(8), 1900187.
165 S. R. Shin, *et al.*, Reduced graphene oxide–gelMA hybrid hydrogels as scaffolds for cardiac tissue engineering, *Small*, 2016, **12**(27), 3677–3689.
166 A. Sen Gupta, Nanomedicine approaches in vascular disease: A review, *Nanomedicine*, 2011, **7**(6), 763–779, DOI: 10.1016/j.nano.2011.04.001.
167 C. Spadaccio, *et al.*, Preventing treatment failures in coronary artery disease: what can we learn from the biology of in-stent restenosis, vein graft failure and internal thoracic arteries? Coronary artery disease: preventing graft failure, *Cardiovasc. Res.*, 2020, **116**(3), 505–519, DOI: 10.1093/cvr/cvz214/5545542.
168 R. Holzer, *et al.*, Stenting of aortic coarctation: Acute, intermediate, and long–term results of a prospective multi–institutional registry—Congenital Cardiovascular Interventional Study Consortium (CCISC), *Catheter. Cardiovasc. Interv.*, 2010, **76**(4), 553–563.
169 F. Gao, *et al.*, Layer-by-layer deposition of bioactive layers on magnesium alloy stent materials to improve corrosion resistance and biocompatibility, *Bioact. Mater.*, 2020, **5**(3), 611–623, DOI: 10.1016/j.bioactmat.2020.04.016.
170 R. Podila, T. Moore, F. Alexis and A. M. Rao, Graphene coatings for enhanced hemo-compatibility of nitinol stents, *RSC Adv.*, 2013, **3**(6), 1660–1665, DOI: 10.1039/c2ra23073a.
171 V. Berry, Impermeability of graphene and its applications, *Carbon*, 2013, **62**, 1–10.
172 W. Tsai, J. M. Grunkemeier, C. D. McFarland and T. A. Horbett, Platelet adhesion to polystyrene–based surfaces preadsorbed with plasmas selectively depleted in fibrinogen, fibronectin, vitronectin, or von Willebrand's factor, *J. Biomed. Mater. Res.*, 2002, **60**(3), 348–359.
173 L. Zhang, *et al.*, The influence of surface chemistry on adsorbed fibrinogen conformation, orientation, fiber formation and platelet adhesion, *Acta Biomater.*, 2017, **54**, 164–174.
174 O. Ros, *et al.*, SponGee: a genetic tool for subcellular and cell-specific cGMP manipulation, *Cell Rep.*, 2019, **27**(13), 4003–4012.
175 Z. Yang, *et al.*, Nitric oxide producing coating mimicking endothelium function for multifunctional vascular stents, *Biomaterials*, 2015, **63**, 80–92.
176 H. Zhang, *et al.*, Catechol/polyethyleneimine conversion coating with enhanced corrosion protection of magnesium alloys: potential applications for vascular implants, *J. Mater. Chem. B*, 2018, **6**(43), 6936–6949.
177 G. Liu, *et al.*, A VEGF delivery system targeting MI improves angiogenesis and cardiac function based on the tropism of MSCs and layer-by-layer self-assembly, *Biomaterials*, 2017, **127**, 117–131.
178 A. W. Carpenter and M. H. Schoenfisch, Nitric oxide release: Part II, Therapeutic applications, *Chem. Soc. Rev.*, 2012, **41**(10), 3742–3752.
179 A. de Mel, F. Murad and A. M. Seifalian, Nitric oxide: a guardian for vascular grafts?, *Chem. Rev.*, 2011, **111**(9), 5742–5767.
180 D. J. Suchyta, H. Handa and M. E. Meyerhoff, A nitric oxide-releasing heparin conjugate for delivery of a combined antiplatelet/anticoagulant agent, *Mol. Pharm.*, 2014, **11**(2), 645–650.
181 H. Qiu, *et al.*, Biomimetic engineering endothelium-like coating on cardiovascular stent through heparin and

nitric oxide-generating compound synergistic modification strategy, *Biomaterials*, 2019, **207**, 10–22.
182 K. Veerubhotla and C. H. Lee, Design of biodegradable 3D-printed cardiovascular stent, *Bioprinting*, 2022, **26**, e00204, DOI: 10.1016/j.bprint.2022.e00204.
183 T. Wallerath, *et al.*, Resveratrol, a polyphenolic phytoalexin present in red wine, enhances expression and activity of endothelial nitric oxide synthase, *Circulation*, 2002, **106**(13), 1652–1658.
184 Z. Ungvari, *et al.*, Resveratrol increases vascular oxidative stress resistance, *Am. J. Physiol.: Heart Circ. Physiol.*, 2007, **292**(5), H2417–H2424.
185 J. Li and D. J. Mooney, Designing hydrogels for controlled drug delivery, *Nat. Rev. Mater.*, 2016, **1**(12), 1–17.
186 E. He, S. Serpelloni, P. Alvear, M. Rahimi and F. Taraballi, Vascular Graft Infections: An Overview of Novel Treatments Using Nanoparticles and Nanofibers, *Fibers*, 2022, **10**(2), 12, DOI: 10.3390/fib10020012.
187 A. T. Pereira, *et al.*, Graphene Oxide Coating Improves the Mechanical and Biological Properties of Decellularized Umbilical Cord Arteries, *ACS Appl. Mater. Interfaces*, 2021, **13**(28), 32662–32672, DOI: 10.1021/acsami.1c04028.
188 D. Huo, *et al.*, Construction of Antithrombotic Tissue-Engineered Blood Vessel via Reduced Graphene Oxide Based Dual-Enzyme Biomimetic Cascade, *ACS Nano*, 2017, **11**(11), 10964–10973, DOI: 10.1021/acsnano.7b04836.
189 V. Srimaneepong, H. E. Skallevold, Z. Khurshid, M. S. Zafar, D. Rokaya and J. Sapkota, Graphene for antimicrobial and coating application, *Int. J. Mol. Sci.*, 2022, **23**(1), 499, DOI: 10.3390/ijms23010499.
190 K. H. Schneider, *et al.*, Decellularized human placenta chorion matrix as a favorable source of small-diameter vascular grafts, *Acta Biomater.*, 2016, **29**, 125–134.
191 C.-H. Lin, K. Hsia, H. Ma, H. Lee and J.-H. Lu, In vivo performance of decellularized vascular grafts: a review article, *Int. J. Mol. Sci.*, 2018, **19**(7), 2101.
192 S. Pashneh-Tala, S. MacNeil and F. Claeyssens, The tissue-engineered vascular graft—past, present, and future, *Tissue Eng., Part B*, 2016, **22**(1), 68–100.
193 G. Konig, *et al.*, Mechanical properties of completely autologous human tissue engineered blood vessels compared to human saphenous vein and mammary artery, *Biomaterials*, 2009, **30**(8), 1542–1550.
194 N. Slepičková Kasálková, S. Rimpelová, C. Vacek, *et al.*, Surface activation of Hastalex by vacuum argon plasma for cytocompatibility enhancement., *Heliyon*, 2024, **10**(6), e27816, DOI: 10.1016/j.heliyon.2024.e27816.
195 K. Hammermeister, G. K. Sethi, W. G. Henderson, F. L. Grover, C. Oprian and S. H. Rahimtoola, Outcomes 15 years after valve replacement with a mechanical versus a bioprosthetic valve: final report of the Veterans Affairs randomized trial, *J. Am. Coll. Cardiol.*, 2000, **36**(4), 1152–1158.
196 W. R. E. Jamieson, *et al.*, Performance of bioprostheses and mechanical prostheses assessed by composites of valve-related complications to 15 years after mitral valve replacement, *J. Thorac. Cardiovasc. Surg.*, 2005, **129**(6), 1301–1308.
197 Y. Misawa, Valve-related complications after mechanical heart valve implantation, *Surg. Today*, 2015, **45**(10), 1205–1209.
198 S. Lee, *et al.*, Calcification and oxidative modifications are associated with progressive bioprosthetic heart valve dysfunction, *J. Am. Heart Assoc.*, 2017, **6**(5), e005648.
199 R. A. Manji, B. Ekser, A. H. Menkis and D. K. C. Cooper, Bioprosthetic heart valves of the future, *Xenotransplantation*, 2014, **21**(1), 1–10.
200 D. Bezuidenhout, D. F. Williams and P. Zilla, Polymeric heart valves for surgical implantation, catheter-based technologies and heart assist devices, *Biomaterials*, 2015, **36**, 6–25.
201 A. G. Kidane, *et al.*, Current developments and future prospects for heart valve replacement therapy, *J. Biomed. Mater. Res., Part B*, 2009, **88**(1), 290–303, DOI: 10.1002/jbm.b.31151.
202 Y. Chang, *et al.*, In vitro toxicity evaluation of graphene oxide on A549 cells, *Toxicol. Lett.*, 2011, **200**(3), 201–210.
203 G. Qu, *et al.*, Graphene oxide induces toll-like receptor 4 (TLR4)-dependent necrosis in macrophages, *ACS Nano*, 2013, **7**(7), 5732–5745.
204 S. Goenka, V. Sant and S. Sant, Graphene-based nanomaterials for drug delivery and tissue engineering, *J. Controlled Release*, 2014, **173**, 75–88.
205 E. A. Ovcharenko, *et al.*, A New Nanocomposite Copolymer Based On Functionalised Graphene Oxide for Development of Heart Valves, *Sci. Rep.*, 2020, **10**(1), 5271, DOI: 10.1038/s41598-020-62122-8.
206 A. Owhal, M. Choudhary, A. D. Pingale, S. U. Belgamwar, S. Mukherjee and J. S. Rathore, Non-cytotoxic zinc/f-graphene nanocomposite for tunable degradation and superior tribo-mechanical properties: Synthesized via modified electro co-deposition route, *Mater. Today Commun.*, 2023, **34**, 105112, DOI: 10.1016/j.mtcomm.2022.105112.
207 Z. Zhao, *et al.*, Strengthened corrosion control of biodegradable poly(trimethylene carbonate) coating on bioabsorbable Mg alloy by introducing graphene oxide, *Surf. Coat. Technol.*, 2022, **451**, 129052, DOI: 10.1016/j.surfcoat.2022.129052.
208 C. Pan, *et al.*, Immobilization of bioactive complex on the surface of magnesium alloy stent material to simultaneously improve anticorrosion, hemocompatibility and antibacterial activities, *Colloids Surf., B*, 2021, **199**, 111541, DOI: 10.1016/j.colsurfb.2020.111541.
209 M. C. Yang, *et al.*, Electrochemical polymerization of PEDOT-graphene oxide-heparin composite coating for anti-fouling and anti-clotting of cardiovascular stents, *Polymers*, 2019, **11**(9), 1520, DOI: 10.3390/polym11091520.
210 S. Ge, *et al.*, Inhibition of in-stent restenosis after graphene oxide double-layer drug coating with good biocompatibility, *Regener. Biomater.*, 2019, **6**(5), 299–309, DOI: 10.1093/rb/rbz010.

211 K. Somszor, *et al.*, Personalized, Mechanically Strong, and Biodegradable Coronary Artery Stents via Melt Electrowriting, *ACS Macro Lett.*, 2020, **9**(12), 1732–1739, DOI: 10.1021/acsmacrolett.0c00644.

212 A. M. ElSawy, N. F. Attia, H. I. Mohamed, M. Mohsen and M. H. Talaat, Innovative coating based on graphene and their decorated nanoparticles for medical stent applications, *Mater. Sci. Eng., C*, 2019, **96**, 708–715, DOI: 10.1016/j.msec.2018.11.084.

213 M. Wawrzyńska, *et al.*, Biocompatible Carbon-Based Coating as Potential Endovascular Material for Stent Surface, *BioMed Res. Int.*, 2018, **1**(2018), 2758347, DOI: 10.1155/2018/2758347.

214 C. J. Pan, *et al.*, Anticoagulation and endothelial cell behaviors of heparin-loaded graphene oxide coating on titanium surface, *Mater. Sci. Eng., C*, 2016, **63**, 333–340, DOI: 10.1016/j.msec.2016.03.001.

215 X. Jing, H. Y. Mi, M. R. Salick, T. M. Cordie, X. F. Peng and L. S. Turng, Electrospinning thermoplastic polyurethane/graphene oxide scaffolds for small diameter vascular graft applications, *Mater. Sci. Eng., C*, 2015, **49**, 40–50, DOI: 10.1016/j.msec.2014.12.060.

216 S. Karimi Alavije, M. Kokabi and M. Soleimani, Endothelial cells performance on 3D electrospun PVA/graphene nanocomposite tubular scaffolds, *Polym. Bull.*, 2021, **78**(9), 4797–4815, DOI: 10.1007/s00289-020-03340-y.

217 W. Najahi-Missaoui, R. D. Arnold and B. S. Cummings, Safe nanoparticles: are we there yet?, *Int. J. Mol. Sci.*, 2020, **22**(1), 385.

218 S. Medici, M. Peana, A. Pelucelli and M. A. Zoroddu, An updated overview on metal nanoparticles toxicity, in *Seminars in cancer biology*, Elsevier, 2021, pp. 17–26.

219 C. McCallion, J. Burthem, K. Rees-Unwin, A. Golovanov and A. Pluen, Graphene in therapeutics delivery: Problems, solutions and future opportunities, *Eur. J. Pharm. Biopharm.*, 2016, **104**, 235–250.

220 J. Han, *et al.*, Dual roles of graphene oxide to attenuate inflammation and elicit timely polarization of macrophage phenotypes for cardiac repair, *ACS Nano*, 2018, **12**(2), 1959–1977.

221 K. Ghosal, P. Mondal, S. Bera and S. Ghosh, Graphene family nanomaterials-opportunities and challenges in tissue engineering applications, *FlatChem*, 2021, **30**, 100315.

222 S. K. Singh, M. K. Singh, P. P. Kulkarni, V. K. Sonkar, J. J. A. Grácio and D. Dash, Amine-modified graphene: thrombo-protective safer alternative to graphene oxide for biomedical applications, *ACS Nano*, 2012, **6**(3), 2731–2740.

223 X. Zhang, *et al.*, Distribution and biocompatibility studies of graphene oxide in mice after intravenous administration, *Carbon*, 2011, **49**(3), 986–995.

224 L. Ou, *et al.*, Toxicity of graphene-family nanoparticles: a general review of the origins and mechanisms, *Part. Fibre Toxicol.*, 2016, **13**(1), 1–24.

225 A. T. Pereira, *et al.*, Graphene-based materials: The key for the successful application of pHEMA as a blood-contacting device, *Biomater. Sci.*, 2021, **9**(9), 3362–3377.

226 C. N. R. Rao and A. K. Sood, *Graphene: synthesis, properties, and phenomena*, John Wiley & Sons, 2013.

227 S. K. Singh, *et al.*, Thrombus inducing property of atomically thin graphene oxide sheets, *ACS Nano*, 2011, **5**(6), 4987–4996.

228 J. Mu, F. Gao, G. Cui, S. Wang, S. Tang and Z. Li, A comprehensive review of anticorrosive graphene-composite coatings, *Prog. Org. Coat.*, 2021, **157**, 106321.

229 M. Schriver, W. Regan, W. J. Gannett, A. M. Zaniewski, M. F. Crommie and A. Zettl, Graphene as a long-term metal oxidation barrier: worse than nothing, *ACS Nano*, 2013, **7**(7), 5763–5768.

230 A. C. Ferrari, *et al.*, Science and technology roadmap for graphene, related two-dimensional crystals, and hybrid systems, *Nanoscale*, 2015, **7**(11), 4598–4810.

231 A. Sasidharan, *et al.*, Comparative in vivo toxicity, organ biodistribution and immune response of pristine, carboxylated and PEGylated few-layer graphene sheets in Swiss albino mice: A three month study, *Carbon*, 2015, **95**, 511–524.

232 X. Tan, *et al.*, Functionalization of graphene oxide generates a unique interface for selective serum protein interactions, *ACS Appl. Mater. Interfaces*, 2013, **5**(4), 1370–1377.

233 E. Demirel and Y. Y. Durmaz, PEGylated reduced graphene oxide as nanoplatform for targeted gene and drug delivery, *Eur. Polym. J.*, 2023, **186**, 111841.

234 F. Liu, Y. Sun, C. Kang and H. Zhu, Pegylated drug delivery systems: from design to biomedical applications, *Nano LIFE*, 2016, **6**(03n04), 1642002.

235 M. Aleemardani, L. Johnson, M. Z. Trikić, N. H. Green and F. Claeyssens, Synthesis and characterisation of photocurable poly (glycerol sebacate)-co-poly (ethylene glycol) methacrylates, *Mater. Today Adv.*, 2023, **19**, 100410.

236 R. K. Thapa, Y. S. Youn, J.-H. Jeong, H.-G. Choi, C. S. Yong and J. O. Kim, Graphene oxide-wrapped PEGylated liquid crystalline nanoparticles for effective chemo-photothermal therapy of metastatic prostate cancer cells, *Colloids Surf., B*, 2016, **143**, 271–277.

237 M. Xu, *et al.*, Improved in vitro and in vivo biocompatibility of graphene oxide through surface modification: poly (acrylic acid)-functionalization is superior to PEGylation, *ACS Nano*, 2016, **10**(3), 3267–3281.

238 E. Demirel, E. Karaca and Y. Y. Durmaz, Effective PEGylation method to improve biocompatibility of graphene derivatives, *Eur. Polym. J.*, 2020, **124**, 109504.

239 E. A. Chiticaru and M. Ionita, Graphene toxicity and future perspectives in healthcare and biomedicine, *FlatChem*, 2022, **35**, 100417.

240 C. Xu, *et al.*, Long circulating reduced graphene oxide–iron oxide nanoparticles for efficient tumor targeting and multimodality imaging, *Nanoscale*, 2016, **8**(25), 12683–12692.

241 H.-J. Im, *et al.*, Accelerated blood clearance phenomenon reduces the passive targeting of PEGylated nanoparticles in peripheral arterial disease, *ACS Appl. Mater. Interfaces*, 2016, **8**(28), 17955–17963.
242 C. G. England, *et al.*, Re-assessing the enhanced permeability and retention effect in peripheral arterial disease using radiolabeled long circulating nanoparticles, *Biomaterials*, 2016, **100**, 101–109.
243 R. Kumar, *et al.*, Graphene-based materials for biotechnological and biomedical applications: Drug delivery, bioimaging and biosensing, *Mater. Today Adv.*, 2023, **33**, 101750.
244 Z. Gao, S. Qin, C. Ménard-Moyon and A. Bianco, Applications of graphene-based nanomaterials in drug design: The good, the bad and the ugly, *Expert Opin. Drug Discovery*, 2023, **18**(12), 1321–1332.
245 N. Baheiraei, M. Razavi and R. Ghahremanzadeh, Reduced graphene oxide coated alginate scaffolds: potential for cardiac patch application, *Biomater. Res.*, 2023, **27**(1), 109.
246 C.-H. Kim, S.-Y. Lee, K. Y. Rhee and S.-J. Park, Carbon-based composites in biomedical applications: a comprehensive review of properties, applications, and future directions, *Adv. Compos. Hybrid Mater.*, 2024, **7**(2), 55.
247 Z. Niknam, *et al.*, Recent advances and challenges in graphene–based nanocomposite scaffolds for tissue engineering application, *J. Biomed. Mater. Res., Part A*, 2022, **110**(10), 1695–1721.
248 X. Jing, H. Y. Mi, B. N. Napiwocki, X. F. Peng and L. S. Turng, Mussel-inspired electroactive chitosan/graphene oxide composite hydrogel with rapid self-healing and recovery behavior for tissue engineering, *Carbon*, 2017, **125**, 557–570, DOI: **10.1016/j.carbon.2017.09.071**.
249 C. J. Bullock and C. Bussy, Biocompatibility considerations in the design of graphene biomedical materials, *Adv. Mater. Interfaces*, 2019, **6**(11), 1900229.
250 J. Lee, *et al.*, Nanoparticle-based hybrid scaffolds for deciphering the role of multimodal cues in cardiac tissue engineering, *ACS Nano*, 2019, **13**(11), 12525–12539.
251 H. Kaur, *et al.*, Progress and challenges of graphene and its congeners for biomedical applications, *J. Mol. Liq.*, 2022, **368**, 120703.
252 A. N. Banerjee, Graphene and its derivatives as biomedical materials: Future prospects and challenges, *Interface Focus*, 2018, **8**(3), 20170056.
253 P. Orsu and A. Koyyada, Recent progresses and challenges in graphene based nano materials for advanced therapeutical applications: a comprehensive review, *Mater. Today Commun.*, 2020, **22**, 100823.
254 K. S. Novoselov, L. Colombo, P. R. Gellert, M. G. Schwab and K. Kim, A roadmap for graphene, *Nature*, 2012, **490**(7419), 192–200.